HHS Public Access

Author manuscript

Sci Transl Med. Author manuscript; available in PMC 2019 July 08.

Published in final edited form as:

Sci Transl Med. 2018 July 04; 10(448): . doi:10.1126/scitranslmed.aar2238.

BCL3 expression promotes resistance to alkylating chemotherapy in gliomas

Longtao Wu[1], **Giovanna M. Bernal**[1], **Kirk E. Cahill**[1], **Peter Pytel**[2], **Carrie A. Fitzpatrick**[2], **Heather Mashek**[2], **Ralph R. Weichselbaum**[3], and **Bakhtiar Yamini**[1,*]

[1]Section of Neurosurgery, Department of Surgery, University of Chicago, Chicago, IL 60637, USA.

[2]Department of Pathology, University of Chicago, Chicago, IL 60637, USA.

[3]Department of Radiation and Cellular Oncology and the Ludwig Center for Metastasis Research, University of Chicago, Chicago, IL 60637, USA.

Abstract

The response of patients with gliomas to alkylating chemotherapy is heterogeneous. However, there are currently no universally accepted predictors of patient response to these agents. We identify the nuclear factor κB (NF-κB) co-regulator B cell CLL/lymphoma 3 (BCL-3) as an independent predictor of response to temozolomide (TMZ) treatment. In glioma patients with tumors that have a methylated O^6-methylguanine DNA methyltransferase (*MGMT*) promoter, high BCL-3 expression was associated with a poor response to TMZ. Mechanistically, BCL-3 promoted a more malignant phenotype by inducing an epithelial-to-mesenchymal transition in glioblastomas through promoter-specific NF-κB dimer exchange. Carbonic anhydrase II (CAII) was identified as a downstream factor promoting BCL-3–mediated resistance to chemotherapy. Experiments in glioma xenograft mouse models demonstrated that the CAII inhibitor acetazolamide enhanced survival of TMZ-treated animals. Our data suggest that BCL-3 might be a useful indicator of glioma response to alkylating chemotherapy and that acetazolamide might be repurposed as a chemosensitizer for treating TMZ-resistant gliomas.

[*]Corresponding author. byamini@surgery.bsd.uchicago.edu.

Author contributions: L.W. performed all of the in vitro and xenograft experiments except as indicated below, analyzed all the clinical data sets including all multivariate and statistical analyses, analyzed experimental data, and edited the manuscript; G.M.B. performed two xenograft experiments with U87 cells and one with GBM43S cells; K.E.C. helped perform in vitro si-*BCL3* array experiment; P.P. performed IHC analysis; C.A.F. and H.M. made FISH probes and performed FISH studies; R.R.W. edited the manuscript; B.Y. conceived and planned the research, helped perform IHC and FISH studies, analyzed the data, and wrote the manuscript.

SUPPLEMENTARY MATERIALS

www.sciencetranslationalmedicine.org/cgi/content/full/10/448/eaar2238/DC1

Competing interests: The authors declare that they have no competing interests.

Data and materials availability: Expression data from microarray studies have been deposited in the National Center for Biotechnology Information Gene Expression Omnibus (accession GSE80729) and are openly available. In addition, data from the publicly available data sets are freely available at the locations cited for each specific database.

INTRODUCTION

Diffuse gliomas encompass both lower-grade gliomas (LGGs), including grade II and III tumors, and glioblastoma (GBM). Within each grade, subgroups of tumors that have significantly different responses to therapy exist (1, 2). Despite this heterogeneity, virtually all glioma patients receive alkylating chemotherapy as part of their treatment regimen. Although alkylators like temozolomide (TMZ) improve overall patient survival (3), many patients experience minimal benefit from their use. These observations underline the critical need for predictors of response to alkylating therapy.

Glioma cells are distinguished by the presence of recurrent copy number alterations (CNAs) affecting broad chromosomal regions (4). Although these alterations primarily involve driver genes, they can also affect nearby passenger genes not directly involved in malignant progression (5). It has been suggested that targeting such flanking genes might have therapeutic effects (6). However, passenger genes, unlike drivers, have not yet been shown to mediate therapeutic susceptibility in clinical glioma (7).

The best described mechanism of resistance to TMZ involves direct cytotoxic lesion repair by the DNA repair enzyme O^6-methylguanine DNA methyltransferase (MGMT) (8). However, even in tumors with low MGMT expression, other pathways have been shown to independently modulate response to therapy and patient outcome (9).

Nuclear factor κB (NF-κB) plays an important role in promoting resistance to DNA-damaging agents in GBM (10, 11). In addition to the five primary NF-κB subunits, p50 (NF-κB1, p105), p52 (NF-κB2, p100), p65 (RelA), RelB, and c-Rel (12), multiple co-regulators also contribute to the overall downstream response. B cell CLL/lymphoma 3 (BCL-3) is an atypical inhibitor κB (IκB) protein that both activates and inhibits NF-κB signaling (13). BCL-3 is a candidate oncoprotein shown to be up-regulated in several malignancies (14, 15) that regulates NF-κB signaling in conjunction with p50- and p52-containing dimers (16-18).

Here, we show that BCL-3 reduced TMZ-induced cytotoxicity in gliomas through the activation of carbonic anhydrase II (CAII). In addition, we found that the CA inhibitor acetazolamide (ACZ) potentiated the effect of TMZ in mouse models of glioma, identifying a potential repurposing strategy for TMZ chemosensitization.

RESULTS

BCL3 is an independent predictor of response to TMZ in GBM

To examine the role of BCL-3 in response to TMZ, we altered its expression in patient-derived glioma stem-like cells (GSCs) (table S1) using vectors expressing human BCL-3 or short hairpins (sh) targeting *BCL3* (fig. S1, A and B). Knockdown of *BCL3* in GSCs with high basal BCL-3 increased cell death after treatment with TMZ (Fig. 1A and fig. S1C). Conversely, overexpression of BCL-3 in GSCs with low basal BCL-3 decreased TMZ-induced death (Fig. 1B and fig. S1D). Moreover, in U87, U251, and T98 GBM cell lines, knockdown of *BCL3* with short interfering RNA (si-RNA) increased the TMZ-induced effect on clonal survival (fig. S1E), whereas overexpression of BCL-3 reduced the efficacy

of TMZ (Fig. 1C and fig. S1F). These findings indicate that BCL-3 modulates cytotoxicity induced by TMZ.

Next, to investigate BCL-3 in clinical GBM, we examined four independent expression databases. In these data sets, patients with high *BCL3* expression had reduced survival compared to patients with low *BCL3* expression (Fig. 1D, fig. S1G, and table S2). *BCL3* expression was significantly associated with survival on multivariate analysis, taking the primary GBM prognostic factors into consideration [hazard ratio (HR), 1.455; $P = 0.017$; Table 1]. The expression of none of the primary NF-κB subunits correlated with survival (fig. S1H). Similarly, *NFKBIA*, the gene encoding IκBα, a potential tumor suppressor in GBM (19), also had no prognostic value on its own (fig. S1I). These results indicate that *BCL3* expression plays an independent role in GBM patient outcome.

To understand whether *BCL3* is specifically relevant in the setting of alkylation damage, we looked at TCGA to analyze whether *BCL3* expression affected survival of GBM patients who were untreated, treated with ionizing radiation (IR) alone, or treated with IR in combination with TMZ. *BCL3* expression did not segregate GBM patients into survival groups if they were untreated or treated with IR alone (Fig. 1E and fig. S1J). Consistent with this latter finding, overexpression of BCL-3 in GBM cells did not alter clonal survival in response to IR (fig. S1K). However, when TMZ was added to IR, patients with low *BCL3* expression survived significantly longer than those with high expression ($P = 0.0084$; Fig. 1E and fig. S1J). In patients treated with TMZ, *BCL3* expression remained associated with survival on multivariate analysis, taking into account *MGMT* promoter methylation, the primary factor associated with resistance to alkylating chemotherapy in GBM (table S3) (8). Moreover, our analysis revealed that addition of TMZ improved survival only in tumors with low *BCL3* expression (Fig. 1E, inset graphs). To validate this role of *BCL3*, we examined a second GBM expression data set, the Repository of Molecular Brain Neoplasia Data (REMBRANDT) (20). In this data set, patients also received procarbazine, lomustine, and vincristine (PCV) as alkylating chemotherapy. In REMBRANDT, *BCL3* expression was only informative of survival in patients whose treatment regimen included alkylating chemotherapy (fig. S1L). These data indicate that *BCL3* expression was not an intrinsic prognostic factor in GBM or informative of response to IR but specifically modulated the response to alkylating chemotherapy.

Given the link between alkylation damage and *MGMT* promoter methylation (8), we divided patients based on *MGMT* promoter methylation, as assessed by the *MGMT*-STP27 model (21). *BCL3* expression only identified distinct survival groups in tumors with high *MGMT* promoter methylation (Fig. 1F). Specifically, in GBM with high *MGMT* promoter methylation, the HR based on *BCL3* expression was greater than in the entire GBM population (1.88 versus 1.41, respectively, univariate Cox regression; Fig. 1F). The data showed that the prognosis of patients with *MGMT* promoter methylated tumors that also had high *BCL3* expression was similar to that in patients with an unmethylated *MGMT* promoter (Fig. 1F).

As public data sets primarily examine mRNA, to study the role of BCL-3 protein, we obtained specimens from a consecutive series of glioma patients. Individual slides and tissue

microarrays (TMAs) were established, and BCL-3 protein was examined by immunohistochemistry (IHC) in 86 confirmed GBMs. IHC grading was performed in a blinded fashion based on a four-tier system that was converted into a binary scale (Fig. 1G). Clinical characteristics are noted (table S4); greater than 90% of patients received TMZ. Data analysis showed that GBM patients with low BCL-3 staining survived significantly longer than those with high staining [$P < 0.0001$; HR, 5.418; 95% confidence interval (CI), 2.747 to 9.647; Fig. 1H], a finding independent of age. These results support the mRNA data and emphasize the importance of BCL-3 protein in modulating the response to alkylation damage.

BCL3 is predictive in all diffuse gliomas

Alkylating chemotherapy is also important in the management of LGGs. Examination of multiple LGG data sets demonstrated that *BCL3* expression separated these patients into distinct survival groups (Fig. 2A, fig. S2A, and table S5). In addition, our analysis showed that there was no difference in *BCL3* expression between grade II and III tumors (fig. S2, B and C). Multivariate analysis that included age, isocitrate dehydrogenase 1 (*IDH1*) mutation, 1p/19q co-deletion, and *MGMT* promoter methylation showed that *BCL3* expression remained associated with survival (Table 2); moreover, *BCL3* separated LGG patients into different survival groups in tumors with high *MGMT* promoter methylation (Fig. 2B). We next partitioned patients by treatment modality. Consistent with a predictive effect, *BCL3* expression was not informative in LGG patients who did not receive an alkylating agent or those treated with IR alone, whereas in patients treated with TMZ (either alone or with PCV) in combination with IR, *BCL3* expression identified distinct survival groups (Fig. 2C). When data from patients treated with alkylating chemotherapy were analyzed on multivariate analysis, low numbers of patients achieving the endpoint of death precluded meaningful statistical analysis (table S6). To validate the predictive nature of *BCL3*, we examined LGGs from REMBRANDT. In this data set, *BCL3* expression was informative of patient survival only in LGG patients who received alkylating chemotherapy, of which >95% included TMZ (fig. S2D). In addition, given the importance of randomized studies for identifying predictive factors, we looked at European Organization for Research and Treatment of Cancer (EORTC) study 26951, a randomized phase III clinical trial that examined addition of alkylating chemotherapy to IR in LGG (22). In this study, performed before TMZ was routinely used, *BCL3* expression was not informative of survival time in patients treated with IR alone. However, among patients who received alkylating chemotherapy in addition to IR, those with low *BCL3* expression survived significantly longer (HR, 2.051; $P < 0.044$; Fig. 2D). Moreover, multivariate analysis among patients that received chemotherapy showed that *BCL3* expression remained significant ($P = 0.006$) when factoring in age and 1p/19q status (table S7; *IDH1* mutation was not included due to incomplete patient data). These findings indicate that *BCL3* is an independent predictor of response to alkylating chemotherapy in LGG.

Given that *IDH* mutation status is as important a prognostic marker as tumor grade (23), we examined a pan-glioma data set (grade II, III, and IV tumors) in which patients were separated by *IDH1* mutation status (24). Notably, *IDH1*-mutant (*IDH*-mt) gliomas had lower *BCL3* expression than *IDH*–wild type (wt) (Fig. 2E). Similar results were seen with CpG

island methylator phenotype (CIMP)–positive tumors compared to CIMP-negative tumors (fig. S2E). Our analysis also showed that *BCL3* expression was reduced in LGG compared to GBM ($P < 0.001$, fig. S2F). In this pan-glioma data set, *BCL3* was correlated with survival on multivariate analysis, taking *IDH1* mutation, *MGMT* methylation, 1p/19q co-deletion, and age into consideration (Table 3). Consistent with a predictive effect, *BCL3* expression separated pan-glioma patients into distinct survival groups only if they received alkylating chemotherapy in their treatment regimen (Fig. 2F). In these patients, *BCL3* expression remained significant ($P = 0.023$) on multivariate analysis incorporating *IDH1* mutation and *MGMT* promoter methylation (table S8). In summary, these data indicate that *BCL3* is an independent predictor of response to alkylating chemotherapy in diffuse gliomas.

BCL3 loss is a passenger event associated with survival

Multiple transcription factors can contribute to *BCL3* mRNA expression (13); however, it is notable that *BCL3* is found on 19q13, a chromosomal band deleted in 20 to 40% of all types of glioma (25-29). We therefore examined the relationship between *BCL3* copy number (CN) and expression. In both LGGs and GBMs, tumors with *BCL3* CN loss had significantly lower *BCL3* mRNA expression ($P < 0.003$; Fig. 3A). Moreover, in an independent data set, LGGs and GBM with 19q deletion had significantly lower *BCL3* expression than nondeleted tumors ($P < 0.01$; Fig. 3B). To examine the link between CN and protein expression, we performed fluorescence in situ hybridization (FISH) on TMA samples. Tumors with hemizygous *BCL3* deletion had significantly lower BCL-3 than nondeleted tumors, as assessed by IHC ($P = 0.0007$; Fig. 3C). The association between CN and *BCL3* expression raised the question of whether CN is also linked to survival. In both LGG and GBM groups, patients who had tumors with *BCL3* deletion survived significantly longer than those with nondeleted tumors ($P < 0.05$; Fig. 3D). Moreover, *BCL3* CN remained significantly associated with survival on multivariate analysis ($P = 0.021$; table S9). These results indicate that genetic deletion of *BCL3* is associated with reduced BCL-3 expression and improved survival.

The prevalence of *BCL3* loss suggests either that *BCL3* is a driver of glioma formation or that it is inadvertently affected by alterations targeted to a large chromosomal region. The lack of reported *BCL3* mutations or translocations in glioma suggested that *BCL3* loss is not a driver of these tumors (fig. S3A). Conversely, CNAs of *BCL3* correlated with those of nearby genes (fig. S3B), suggesting that their CNAs are closely linked. Therefore, we examined the CN status of the genes surrounding *BCL3* in 19q13.31-32. Analysis of TCGA data showed that in both GBM and LGG, loss of all the genes in this band correlated not only with *BCL3* but also with the other genes in the region (Fig. 3E and fig. S3C), suggesting that *BCL3* deletion occurs as a result of modifications targeted to a broad region of 19q13. This finding is consistent not only with the fact that the entire 19q arm is lost in oligodendrogliomas but also with the observation that, in astrocytic tumors and GBM, CNAs within 19q13 involve a broad region (26, 30). The above data support the hypothesis that *BCL3* loss is a passenger event seen in all types of glioma.

Despite the importance of deletion, some *BCL3* nondeleted gliomas also had low mRNA expression. Given the role of epigenetic modifications in regulating expression, we examined *BCL3* promoter methylation. In TCGA pan-glioma data, a significant inverse correlation between *BCL3* promoter methylation and expression was seen ($P < 0.0001$; fig. S3D). Although the correlation was evident in *IDH*-wt and *IDH*-mt tumors, this was stronger in *IDH*-wt tumors (fig. S3D). Analysis of the pan-glioma data set demonstrated that *BCL3* promoter methylation was significantly associated with survival on multivariate analysis incorporating *IDH* mutation, *MGMT* promoter methylation, and 1p/19q co-deletion ($P = 0.018$; table S10). Moreover, when the data were separated by the patients' *IDH* status, *BCL3* promoter methylation was only informative in patients with *IDH*-wt tumors (Fig. 3F), a finding consistent with the stronger correlation between *BCL3* methylation and expression in *IDH*-wt compared to *IDH*-mt tumors (fig. S3D). These results indicate that, in glioma, the genetic and epigenetic alterations of *BCL3* that regulate expression are significantly associated with survival.

Given the correlation between *BCL3* CN loss and that of other 19q13 genes, we examined whether the expression of other 19q13 genes was also associated with survival. Unlike *BCL3*, the mRNA expression of none of the surrounding 19q13 genes (fig. S3C) could separate TCGA GBM patients into significantly distinct survival groups, including the expression of *RELB*, an NF-κB subunit located on 19q13 whose CNAs are tightly linked to *BCL3* and have been previously associated with GBM (fig. S1H) (2, 31) (GlioVis data portal for visualization and analysis of brain tumor expression data sets) (32). These findings indicate that the correlation between *BCL3* loss and survival does not extrapolate to all genes in the 19q13 chromosomal region.

BCL-3 induces epithelial-to-mesenchymal transition in GBM

To understand how BCL-3 promotes resistance to alkylation damage, we modulated its expression in GSCs and GBM cell lines. In A172 cells that have extremely low basal BCL-3, overexpression of BCL-3 for 2 weeks changed the cell morphology to a spindle-like appearance, suggestive of epithelial-to-mesenchymal transition (EMT) (Fig. 4A). To further study this finding, we examined GSCs with low and high basal BCL-3 expression. Overexpression of BCL-3 in GBM44 GSCs and A172 cells increased the expression of several mesenchymal markers, including vimentin (VIM), SNAI1, and TWIST1, and reduced the expression of the epithelial marker E-cadherin (*CDH1*) (Fig. 4B and fig. S4A). Conversely, knockdown of *BCL3* in GSCs expressing high basal BCL-3, GBM43S and GBM34, resulted in decreased mesenchymal marker expression (Fig. 4B). One prominent feature of mesenchymal differentiation is acquisition of a more stem cell–like phenotype (1, 33) that can be demonstrated in vitro by analysis of neurosphere formation. Loss of *BCL3* reduced neurosphere formation ability in GBM34 cells, whereas overexpression of BCL-3 had the opposite effect in GBM44 GSCs, supporting the role of BCL-3 in mesenchymal differentiation (Fig. 4C). Consistent with the above, in TCGA GBM and LGG, a correlation between the expression of *BCL3* and multiple EMT markers was seen (Fig. 4D and fig. S4B). Moreover, mesenchymal (MES) GBMs, as determined by the Phillips or Verhaak classification systems (1, 2), had significantly higher *BCL3* expression than proneural (PN) tumors ($P < 0.005$; Fig. 4E and fig. S4C). Correlation of *BCL3* with the Phillips MES or PN

signature genes (1) demonstrated that, although there was a strong positive correlation between *BCL3* and all the MES signature genes (mean correlation is 0.59, ±0.13; table S11), the correlation between *BCL3* and PN signature genes was negative (mean correlation is −0.39, ±0.17; table S11) (GlioVis data portal for visualization and analysis of brain tumor expression data sets) (32). These data suggest that, in glioma, BCL-3 promotes mesenchymal differentiation.

BCL-3 induces mesenchymal differentiation via promoter-specific NF-κB dimer exchange

BCL-3 has no known enzymatic function and mediates its effects by regulating downstream gene expression. To understand how BCL-3 promotes mesenchymal differentiation, we examined genome-wide mRNA expression in GBM cells expressing si-*BCL3* compared to si-control, a nontargeted sequence (table S12). As BCL-3 primarily acts by modulating NF-κB signaling, we looked at NF-κB–dependent factors previously identified as being specific to the MES phenotype (10). Knockdown of *BCL3* caused a decrease of more than 80% of NF-κB–dependent MES genes (Fig. 5A). Among the transcripts most significantly down-regulated (>2-fold, adjusted $P < 0.001$) were *CD44*, chemokine (C-C motif) ligand 2 (*CCL2*), colony-stimulating factor 2 (*CSF2*), NF-κB–dependent factors critical for mesenchymal differentiation (10), and leukemia inhibitory factor (*LIF*), a primary MES signature gene (1). The BCL-3 dependence of these and several other MES genes was verified after depletion and overexpression of BCL-3 in GSCs and GBM cells (Fig. 5B and fig. S5A). In addition, in clinical GBM, a strong correlation between the expression of these factors and *BCL3* was seen (Fig. 5C).

To study the mechanism by which BCL-3 modulates NF-κB, we first examined an NF-κB–dependent luciferase reporter. Overexpression of BCL-3 in GBM cells caused an increase in basal and tumor necrosis factor–α (TNFα)–induced NF-κB activity (Fig. 5D) and an increase in TNFα-induced CD44 expression (fig. S5B), a finding previously reported to promote mesenchymal differentiation (10). We then looked at the primary NF-κB subunits p50, p52, and p65. Although overexpression of BCL-3 did not induce a change in subunit expression, it increased p65 nuclear translocation (Fig. 5E). To examine this finding further, we depleted *BCL3* in GBM34 GSCs. Knockdown of *BCL3* using two distinct sh-RNA constructs decreased nuclear and increased cytoplasmic p65 (Fig. 5F). Given this finding, to study whether inherent differences in BCL-3 correlated with differences in nuclear p65, we first examined GSCs and GBM cell lines. In the cell lines examined, we found a positive correlation between BCL-3 and nuclear p65 protein (Fig. 5G). In addition, in clinical GBM specimens, we found a significant positive correlation between nuclear IHC staining of BCL-3 and p65 ($P = 0.009$; Fig. 5H). These results suggest that, in GBM, BCL-3 induces NF-κB activity and promotes p65 nuclear translocation.

Although BCL-3 did not alter the amount of nuclear p50 or p52, we examined whether it promoted MES differentiation by altering the chromatin recruitment of these subunits. We performed quantitative chromatin immunoprecipitation (qChIP) using primers spanning the κB sites of several BCL-3–regulated MES genes. Overexpression of BCL-3 induced recruitment of p65 to the κB sites of MES-specific genes, including *CD44* and *LIF* (Fig. 5I and fig. S5C). Also, whereas p50 recruitment decreased at *CD44, LIF*, and *CCL2* promoters,

the recruitment of p52 increased (Fig. 5I and fig. S5C). Gel shift studies using probes corresponding to the *CD44* and *CCL2* κB sites showed that, in the presence of high BCL-3, p50 DNA binding was lost, whereas p52 binding was induced at both κB sites (Fig. 5J and fig. S5D). Finally, we examined endogenous chromatin enrichment of NF-κB subunits at MES promoters in patient-derived GSCs. The predominant subunits bound to MES promoters in GBM34 GSCs (BCL-3 high) were p65 and p52 (Fig. 5K). These findings indicate that high BCL-3 promotes MES gene expression by inducing promoter-specific NF-κB dimer exchange.

The increased recruitment of p52 to MES promoters suggested that p52 is involved in mediating the MES differentiation induced by BCL-3. We therefore depleted p52/*NFKB2* in GBM34 GSCs (BCL-3 high). Knockdown of p52/*NFKB2* resulted in decreased expression of *CD44, CCL2*, and interleukin-8 (*IL8*) (fig. S5E). Moreover, in TCGA GBMs, there was a positive correlation between the expression of *NFKB2* and these MES genes (fig. S5F). In addition, depletion of p52/*NFKB2* not only attenuated basal NF-κB–regulated MES gene expression but also blocked the increase induced by BCL-3 overexpression (fig. S5G). These results indicate that p52 mediates BCL-3–dependent increase in MES gene expression.

CAII mediates BCL-3–dependent resistance to TMZ

The results indicate that BCL-3 is informative specifically in patients treated with alkylating agents such as TMZ. To identify BCL-3–regulated factors that could be responsible for the resistance to TMZ and that could potentially be targeted for inhibition, we examined the gene expression response induced by TMZ, focusing on genes up-regulated by treatment. To screen for differentially expressed transcripts, we depleted *BCL3* in U87 cells, a cell line with moderate BCL-3 expression that was sensitized to TMZ by *BCL3* knockdown. The sole transcript induced by TMZ in the presence of BCL-3 and down-regulated with depletion of *BCL3* was *CAII* (Fig. 6A and tables S12 and S13). CAII was induced by TMZ in GSCs (Fig. 6B and fig. S6A), and BCL-3 was required for this induction (Fig. 6C). Also, in clinical databases, tumors with low *BCL3* expression had lower *CAII* mRNA expression than those with high *BCL3* expression, as did tumors with 19q deletion compared to the nondeleted group (Fig. 6D and fig. S6, B and C). In addition, MES GBMs had higher *CAII* expression than PN tumors (fig. S6D). To examine the relevance of alkyl adducts for induction of CAII by TMZ, we modulated MGMT expression. Knockdown of *MGMT* in GBM26 GSCs (that express high MGMT and BCL-3) increased TMZ-induced *CAII* expression (Fig. 6E), whereas expression of MGMT in GBM cells with no MGMT blocked the effect of TMZ on *CAII* expression (fig. S6E). These findings suggest that TMZ induces CAII via formation of cytotoxic O^6-methylguanine adducts.

No CA isoforms have yet been reported to be NF-κB target genes. Although knockdown of either p50/NFκB1 or p65 did not alter basal *CAII* expression, loss of p52/NFκB2 attenuated basal and TMZ-induced *CAII* expression in GBM34 GSCs (Fig. 6F and fig. S6F). Analysis of the *CAII* promoter and the upstream coding region revealed three potential κB sites (κB1, κB2, and κB3; Fig. 6G). ChIP studies demonstrated that p50, p52, and p65 are recruited to κB1 and κB2, but not κB3, and gel shift analysis showed that NF-κB binds the κB2 probe (fig. S6G). In U87 cells, TMZ decreased enrichment of p50 at κB1 and κB2, increased

enrichment of p52 (Fig. 6H), and had no effect on either BCL-3 or p65 (fig. S6H). Consistent with this, gel shift studies showed that, in response to TMZ, p52 replaced p50 in the NF-κB dimer bound to the κB2 probe (Fig. 6I). The above findings suggested that TMZ modulates the interaction of BCL-3 with p50 and p52. To examine this more closely, we studied GSCs with high BCL-3 expression. Western blot analysis revealed that TMZ reduced the interaction of BCL-3 with p50 and enhanced the association of BCL-3 with p52 (Fig. 6J). Given that TMZ induces phosphorylation of p50 S329 (11) and that S329 is a residue that potentially interacts with BCL-3 (34), we examined the role of this residue in regulating the BCL-3/p50 interaction in response to TMZ. Mutation of S329 to an unphosphorylatable form blocked the dissociation of p50 and BCL-3 after TMZ treatment (Fig. 6K). Together, these findings highlight the importance of the reciprocal interaction of BCL-3 with p50 and p52 for induction of CAII by TMZ.

Finally, to examine whether CAII is involved in the cytotoxicity induced by TMZ, we altered its expression in GSCs and GBM cells. Overexpression of CAII attenuated cell death induced by TMZ (Fig. 6L and fig. S6, I and J), whereas knockdown of *CAII* in GBM26 GSCs led to an increase in TMZ-induced cytotoxicity (Fig. 6M). Moreover, depletion of *CAII* and *BCL3* together did not increase the anti-glioma effect of TMZ any more than knockdown of BCL-3 alone (Fig. 6N), supporting the contention that CAII and BCL-3 act in the same pathway in response to TMZ. These findings indicate that BCL-3 promotes resistance to TMZ by induction of CAII as a result of promoter-specific NF-κB dimer exchange.

ACZ enhances the anti-glioma effect of TMZ

CAII is potently blocked by the CA inhibitor ACZ (35). ACZ has been reported to be effective against GBM cells (36, 37) and to enhance apoptosis by TMZ (38, 39). Consistent with this observation, we found that although ACZ alone did not alter overall clonogenic survival of GBM cells, it enhanced the ability of TMZ to reduce survival (fig. S7A). To study the role of BCL-3 in this response, patient-derived GSCs were examined. ACZ enhanced cytotoxicity by TMZ in GBM34 GSCs that express high BCL-3, and knockdown of *BCL3* blocked the chemosensitizing effect of ACZ (Fig. 7A). In GBM44 GSCs that have low BCL-3 expression, ACZ did not modulate the cytotoxic effect induced by TMZ; however, overexpression of BCL-3 enabled ACZ to enhance cell death by TMZ (Fig. 7B). Similarly, depletion of *BCL3* attenuated the chemosensitizing effect of ACZ on clonogenic assay (fig. S7B). These results indicate that BCL-3 is required for sensitization to TMZ by ACZ.

Although ACZ is possibly the most commonly used CA inhibitor (40), many other CA inhibitors are available that can potentially enhance the efficacy of TMZ (41). We examined two other clinically used general CA inhibitors, methazolamide (MZM) and topiramate (TPM). MZM enhanced cytotoxicity by TMZ in a BCL-3–dependent manner (fig. S7C), whereas the anti-epileptic agent TPM did not (fig. S7D).

Given that ACZ also acts on other CAs, albeit much less effectively (35), we also examined the requirement of CAII for the combination effect of ACZ and TMZ. Knockdown of *CAII* with si-RNA blocked the chemosensitizing effect of ACZ on TMZ (Fig. 7C), and

overexpression of CAII in cells with low basal BCL-3 promoted chemosensitization by ACZ (fig. S7E). Moreover, in U251 GBM cells that do not express CAII, ACZ only chemosensitized these cells to TMZ when CAII was exogenously expressed (Fig. 7, D and E). The efficacy of ACZ in combination with TMZ raised the question of whether ACZ modified NF-κB activity and mesenchymal differentiation. ACZ did not affect TMZ-induced NF-κB inhibitory activity (fig. S7F), and the addition of ACZ also did not induce p65 phosphorylation or alter MES gene expression (fig. S7, G and H).

To examine combination TMZ and ACZ in vivo, we performed intracranial xenograft studies in mice. In a pilot study, U87 tumors were established and ACZ was administered for 10 days after initiation of TMZ treatment. This combination regimen did not result in a significant change in survival. However, 10 days after TMZ initiation, CAII expression was still elevated (fig. S7I), suggesting that ACZ needed to be administered for a longer period of time. We therefore altered our protocol to treat animals with daily ACZ for a total of 21 days. Using this regimen, ACZ significantly increased survival time in combination with TMZ compared to TMZ alone ($P < 0.05$; Fig. 7F and fig. S7J). ACZ alone did not affect survival in this model (Fig. 7F).

Next, we replicated the experiments in more clinically relevant patient-derived xenograft (PDX) models. In GBM34 and GBM43S xenografts that have high BCL-3 expression, addition of ACZ significantly increased survival compared to TMZ alone ($P < 0.05$; Fig. 7G and H). Addition of ACZ to TMZ in GBM43S xenografts resulted in long-term survival of several animals, a finding repeatedly seen in multiple independent experiments (Fig. 7G and fig. S7L). However, in GBM26 PDX that has high MGMT expression, addition of ACZ had no chemosensitizing effect on TMZ despite the presence of BCL-3 in this tumor (fig. S7, K and M). Finally, to specifically examine the requirement of BCL-3 for chemosensitization by ACZ in vivo, we depleted *BCL3* in GBM34 tumors. Whereas expression of a control sh-RNA did not modulate the response in GBM34 tumors, knockdown of *BCL3* completely blocked the ability of ACZ to increase the prosurvival effect of TMZ (Fig. 7I). Together, these data indicate that ACZ, a commonly used CA inhibitor that has no antitumor effect in GBM by itself, sensitized GBM to TMZ in a BCL-3–dependent manner.

DISCUSSION

This work identifies BCL-3 as an indicator of sensitivity to alkylating chemotherapy in GBM. Although *BCL3* expression separated all GBM patients, it is primarily informative in tumors with high *MGMT* promoter methylation. GBM patients with high *MGMT* promoter methylation, who would be expected to respond well to alkylating agents, had similar survival to those with low *MGMT* promoter methylation if they also had high *BCL3* expression. This finding is likely because cytotoxic O^6-methylguanine adducts are required for BCL-3 to promote resistance to TMZ. In the presence of high *MGMT* expression, cytotoxic adducts are repaired before they signal to BCL-3 (fig. S8). BCL-3 was previously found to be elevated in gliomas and related to survival (42); however, in that study, patients with all grades of glioma were analyzed together, precluding determination of prognostic value. Our results indicate that only tumors with low *BCL3* expression will likely benefit

from adding TMZ to IR, an important clinical observation given that TMZ induces deleterious hypermutation that can cause malignant progression (43).

The data demonstrate that, in glioma, *BCL3* expression is regulated by genetic, and epigenetic, modifications and that these alterations are linked to patient outcome. We see that *BCL3* CN loss occurs as a result of modifications targeted to the chromosomal band 19q13. This finding, when considered with the observation that BCL-3 is a candidate oncoprotein that has never been identified as a glioma driver (4), indicates that *BCL3* loss is a passenger event unrelated to glioma formation. Although the ability of passenger events to promote unintended therapeutic susceptibility has been shown in animal models (44, 45), the link between loss of *BCL3* and TMZ susceptibility demonstrates the importance of passenger modification to chemosensitivity in a clinical setting. The effect of *BCL3* deletion in glioma is particularly relevant given that alterations of 19q play an important role in modulating patient outcome in these tumors. Specifically, 19q, with 1p, co-deletion is predictive of response to alkylating chemotherapy in oligodendroglioma (46), whereas loss of 19q13 alone is associated with long-term survival in GBM (29, 47). The most widely accepted hypothesis as to why 19q13 loss is so prevalent in gliomas is that a glioma-specific tumor suppressor is present in the region (48). Although no 19q tumor suppressor has yet been identified in astrocytic tumors or GBM, capicua transcriptional repressor (*CIC*) was recently discovered in oligodendroglioma (49).

Our studies indicate that BCL-3 promotes GBM mesenchymal differentiation, an observation consistent with previous reports linking BCL-3 to EMT (50-52). We find that, in GBM cells, BCL-3 up-regulated EMT markers and that, in clinical GBM, *BCL3* expression correlated strongly with MES signature gene expression. From a mechanistic standpoint, high BCL-3 led to a change in the composition of the NF-κB dimer at MES gene promoters involving replacement of p50 by p52. In addition, BCL-3 induced p65 nuclear translocation, a finding consistent with the known importance of this subunit in MES change (10). Whereas previous work demonstrates a cell-extrinsic pathway for activation of p65 in GBM cells by cytokines released from infiltrating macrophages and microglia (10), genetic and epigenetic regulation of *BCL3* represents mechanisms by which cell-intrinsic pathways also contribute to promoting NF-κB–dependent mesenchymal differentiation.

An important feature of predictors like BCL-3 is that they are also informative in that they can identify pathways to improve treatment response. *MGMT* promoter methylation is one such predictor; however, inhibiting MGMT has not proven to be an effective chemosensitizing strategy clinically (8). Inhibition of BCL-3 is not currently feasible in patients; therefore, we searched for downstream BCL-3–regulated targets and identified CAII as a mediator of BCL-3–dependent resistance to TMZ. Although several factors have previously been reported to contribute to the antiapoptotic effects of BCL-3 (53-55), from a clinical perspective, CAII stands out because it can be effectively inhibited by ACZ. *CAII* mRNA expression is not prognostic in untreated GBM (GlioVis data portal) (32), yet elevated endothelial CAII has been associated with worse outcome in astrocytoma (56). Regardless of these observations, our data demonstrate that it is not basal expression but the induction of CAII by TMZ that is important in modulating response to therapy.

Although we demonstrated the predictive value of *BCL3* in several independent data sets, an important limitation of our study is its retrospective nature. Ultimately, the clinical validity of using BCL-3 as a predictor in GBM will require verification in a prospective randomized trial. In addition, the question of which CA inhibitor is best for clinical use with TMZ will require further analysis. Finally, a mechanistic limitation of our study is that we have yet to determine how BCL-3 promotes p65 nuclear translocation and promoter-specific dimer exchange.

ACZ has not previously been examined in GBM xenografts; however, it was initially shown to promote chemosensitization in murine fibrosarcoma (57). More recently, ACZ was found to promote cytotoxicity of GBM cells in vitro and other cancers in vivo (37-39, 58). Although there has been significant interest in targeting other hypoxia-specific CA isoforms for GBM therapy (41, 59), ACZ is attractive because of its general clinical use and well-tolerated dosing profile (40). Using PDXs, we see that, in GBM, ACZ promoted chemosensitization specifically in the presence of high BCL-3 and low MGMT expression. Our studies suggest that, in the clinical setting, repurposing ACZ might be particularly effective in a subgroup of *MGMT* promoter methylated tumors that have high BCL-3 expression. Given the increase in molecular analysis of gliomas, factors such as BCL-3 might assume an important role in individualizing patient treatment, a strategy occurring with increasing frequency in cancer therapy.

MATERIALS AND METHODS

Study design

The objectives of this study were to examine the role of BCL-3 in the response of glioma to alkylating chemotherapy and to evaluate the use of ACZ as a chemosensitizer in experimental GBM. There are several design aspects relevant in this work. First, to examine the predictive role of *BCL3*, initially, TCGA was examined and the results were subsequently validated in other databases. Numbers of patients included or excluded in each data set are specifically noted in Materials and Methods and in each individual figure panel. To investigate survival based on BCL-3 IHC, we performed an initial power analysis based on the mRNA data from TCGA. This gave $n = 74$ and 32 patients per group, respectively, to have 80% power to detect a significant difference between low and high BCL-3 expression at a two-sided $P < 0.05$. Subsequently, after institutional review board approval, we obtained 86 consecutive GBM samples that had adequate tissue for IHC. Additional patients were not recruited. Patients were excluded from survival analysis if they died before treatment due to infection or massive hemorrhage, if no follow-up was available, or if they initially had an LGG that progressed to GBM. IHC and FISH grading was performed by two independent investigators blinded to diagnosis and to survival.

For animal studies, no statistical method was used to determine sample size. Efforts were made to achieve the scientific goals with the minimum number of animals. A sample size of five to seven animals per group was chosen on the basis of our previous experience using intracranial PDX GBMs, where we have observed 100% tumor engraftment success. After tumor implantation and before treatment, animals were randomized into the different treatment groups. Animals were excluded from the study if they were sacrificed before

treatment/randomization. Determination of the survival time was performed blinded to the specific treatment group. Experiments were repeated by more than one individual to ensure reproducibility. The survival endpoint was reached when mice lost at least 20% body weight or showed symptoms of neurological deficit. Raw data are located in table S17.

Statistical analysis

Data analysis was performed using Stata/IC 13.0 statistical software (Stata Corporation, licensed to the University of Chicago, Research Computing Center). The Cox proportional hazard model was used for both univariate and multivariate analyses using the specific covariates noted in Results. For survival studies, Kaplan-Meier curves were plotted, and the log-rank test was performed for comparison of cohorts. HR and 95% CIs were calculated using the Mantel-Haenszel estimator model. For analysis of 19q CN correlation, correlation matrix analysis was used, and the R/corrplot package was used to display the correlation matrix. For box-and-whisker graphs, boxes show median and 25th and 75th percentiles, whereas whiskers show the 5th and 95th percentiles analyzed by unpaired *t* test. In vitro and other studies as indicated were analyzed by two-tailed Student's *t* test with significance taken as $P < 0.05$. Pearson correlation was also analyzed by two-tailed Student's *t* test.

Supplementary Material

Refer to Web version on PubMed Central for supplementary material.

Acknowledgments:

We thank the University of Chicago Research Computing Center for support, the University of Chicago and Jonathon Hobbs for assistance with making and staining TMAs, L. Zhang for biostatistical assistance, and A. Uppal.

Funding: This work was supported by NIH grant R01CA136937 to B.Y. and the Ludwig Center for Metastasis Research; K.E.C. was a Howard Hughes Medical Institute Research Fellow.

REFERENCES AND NOTES

1. Phillips HS, Kharbanda S, Chen R, Forrest WF, Soriano RH, Wu TD, Misra A, Nigro JM, Colman H, Soroceanu L, Williams PM, Modrusan Z, Feuerstein BG, Aldape K, Molecular subclasses of high-grade glioma predict prognosis, delineate a pattern of disease progression, and resemble stages in neurogenesis. Cancer Cell 9, 157–173 (2006). [PubMed: 16530701]
2. Verhaak RGW, Hoadley KA, Purdom E, Wang V, Qi Y, Wilkerson MD, Miller CR, Ding L, Golub T, Mesirov JP, Alexe G, Lawrence M, O'Kelly M, Tamayo P, Weir BA, Gabriel S, Winckler W, Gupta S, Jakkula L, Feiler HS, Hodgson JG, James CD, Sarkaria JN, Brennan C, Kahn A, Spellman PT, Wilson RK, Speed TP, Gray JW, Meyerson M, Getz G, Perou CM, Hayes DN; Cancer Genome Atlas Research Network, Integrated genomic analysis identifies clinically relevant subtypes of glioblastoma characterized by abnormalities in PDGFRA, IDH1, EGFR, and NF1. Cancer Cell 17, 98–110 (2010). [PubMed: 20129251]
3. Stupp R, Mason WP, van den Bent MJ, Weller M, Fisher B, Taphoorn MJB, Belanger K, Brandes AA, Marosi C, Bogdahn U, Curschmann J, Janzer RC, Ludwin SK, Gorlia T, Allgeier A, Lacombe D, Cairncross JG, Eisenhauer E, Mirimanoff RO; European Organisation for Research and Treatment of Cancer Brain Tumor and Radiotherapy Groups; National Cancer Institute of Canada Clinical Trials Group, Radiotherapy plus concomitant and adjuvant temozolomide for glioblastoma. N. Engl. J. Med 352, 987–996 (2005). [PubMed: 15758009]

4. Brennan CW, Verhaak RGW, McKenna A, Campos B, Noushmehr H, Salama SR, Zheng S, Chakravarty D, Sanborn JZ, Berman SH, Beroukhim R, Bernard B, Wu C-J, Genovese G, Shmulevich I, Barnholtz-Sloan J, Zou L, Vegesna R, Shukla SA, Ciriello G, Yung WK, Zhang W, Sougnez C, Mikkelsen T, Aldape K, Bigner DD, Van Meir EG, Prados M, Sloan A, Black KL, Eschbacher J, Finocchiaro G, Friedman W, Andrews DW, Guha A, Iacocca M, O'Neill BP, Foltz G, Myers J, Weisenberger DJ, Penny R, Kucherlapati R, Perou CM, Hayes DN, Gibbs R, Marra M, Mills GB, Lander E, Spellman P, Wilson R, Sander C, Weinstein J, Meyerson M, Gabriel S, Laird PW, Haussler D, Getz G, Chin L; TCGA Research Network, The somatic genomic landscape of glioblastoma. Cell 155, 462–477 (2013). [PubMed: 24120142]
5. Masayesva BG, Ha P, Garrett-Mayer E, Pilkington T, Mao R, Pevsner J, Speed T, Benoit N, Moon C-S, Sidransky D, Westra WH, Califano J, Gene expression alterations over large chromosomal regions in cancers include multiple genes unrelated to malignant progression. Proc. Natl. Acad. Sci. U.S.A 101, 8715–8720 (2004). [PubMed: 15155901]
6. Frei III E, Gene deletion: A new target for cancer chemotherapy. Lancet 342, 662–664 (1993). [PubMed: 8103151]
7. Tanaka S, Louis DN, Curry WT, Batchelor TT, Dietrich J, Diagnostic and therapeutic avenues for glioblastoma: No longer a dead end? Nat. Rev. Clin. Oncol 10, 14–26 (2013). [PubMed: 23183634]
8. Hegi ME, Liu L, Herman JG, Stupp R, Wick W, Weller M, Mehta MP, Gilbert MR, Correlation of O^6-methylguanine methyltransferase (MGMT) promoter methylation with clinical outcomes in glioblastoma and clinical strategies to modulate MGMT activity. J. Clin. Oncol 26, 4189–4199 (2008). [PubMed: 18757334]
9. Murat A, Migliavacca E, Gorlia T, Lambiv WL, Shay T, Hamou M-F, de Tribolet N, Regli L, Wick W, Kouwenhoven MCM, Hainfellner JA, Heppner FL, Dietrich P-Y, Zimmer Y, Cairncross JG, Janzer R-C, Domany E, Delorenzi M, Stupp R, Hegi ME, Stem cell–related "self-renewal" signature and high epidermal growth factor receptor expression associated with resistance to concomitant chemoradiotherapy in glioblastoma. J. Clin. Oncol 26, 3015–3024 (2008). [PubMed: 18565887]
10. Bhat KPL, Balasubramaniyan V, Vaillant B, Ezhilarasan R, Hummelink K, Hollingsworth F, Wani K, Heathcock L, James JD, Goodman LD, Conroy S, Long L, Lelic N, Wang S, Gumin J, Raj D, Kodama Y, Raghunathan A, Olar A, Joshi K, Pelloski CE, Heimberger A, Kim SH, Cahill DP, Rao G, Den Dunnen WFA, Boddeke HWGM, Phillips HS, Nakano I, Lang FF, Colman H, Sulman EP, Aldape K, Mesenchymal differentiation mediated by NF-κB promotes radiation resistance in glioblastoma. Cancer Cell24, 331–346 (2013). [PubMed: 23993863]
11. Schmitt AM, Crawley CD, Kang S, Raleigh DR, Yu X, Wahlstrom JS, Voce DJ, Darga TE, Weichselbaum RR, Yamini B, p50 (NF-κB1) is an effector protein in the cytotoxic response to DNA methylation damage. Mol. Cell 44, 785–796 (2011). [PubMed: 22152481]
12. Cahill KE, Morshed RA, Yamini B, Nuclear factor-κB in glioblastoma: Insights into regulators and targeted therapy. Neuro Oncol. 18, 329–339 (2016). [PubMed: 26534766]
13. Palmer S, Chen YH, Bcl-3, a multifaceted modulator of NF-κB-mediated gene transcription. Immunol. Res 42, 210–218 (2008). [PubMed: 19002607]
14. Cogswell PC, Guttridge DC, Funkhouser WK, Baldwin AS Jr., Selective activation of NF-kappa B subunits in human breast cancer: Potential roles for NF-kappa B2/p52 and for Bcl-3. Oncogene 19, 1123–1131 (2000). [PubMed: 10713699]
15. Thornburg NJ, Pathmanathan R, Raab-Traub N, Activation of nuclear factor-κB p50 homodimer/Bcl-3 complexes in nasopharyngeal carcinoma. Cancer Res. 63, 8293–8301 (2003). [PubMed: 14678988]
16. Fujita T, Nolan GP, Liou HC, Scott ML, Baltimore D, The candidate proto-oncogene bcl-3 encodes a transcriptional coactivator that activates through NF-kappa B p50 homodimers. Genes Dev. 7, 1354–1363 (1993). [PubMed: 8330739]
17. Bours V, Franzoso G, Azarenko V, Park S, Kanno T, Brown K, Siebenlist U, The oncoprotein Bcl-3 directly transactivates through kappa B motifs via association with DNA-binding p50B homodimers. Cell 72, 729–739 (1993). [PubMed: 8453667]
18. Wang VY-F, Li Y, Kim D, Zhong X, Du Q, Ghassemian M, Ghosh G, Bcl3 phosphorylation by Akt, Erk2, and IKK is required for its transcriptional activity. Mol. Cell 67, 484–497.e5 (2017). [PubMed: 28689659]

19. Bredel M, Scholtens DM, Yadav AK, Alvarez AA, Renfrow JJ, Chandler JP, Yu ILY, Carro MS, Dai F, Tagge MJ, Ferrarese R, Bredel C, Phillips HS, Lukac PJ, Robe PA, Weyerbrock AVogel H, Dubner S, Mobley B, He X, Scheck AC, Sikic BI, Aldape KD, Chakravarti A, Harsh GR IV, NFKBIA deletion in glioblastomas. N. Engl. J. Med 364, 627–637 (2011). [PubMed: 21175304]

20. Madhavan S, Zenklusen J-C, Kotliarov Y, Sahni H, Fine HA, Buetow K, Rembrandt: Helping personalized medicine become a reality through integrative translational research. Mol. Cancer Res 7, 157–167 (2009). [PubMed: 19208739]

21. Bady P, Sciuscio D, Diserens A-C, Bloch J, van den Bent MJ, Marosi C, Dietrich P-Y, Weller M, Mariani L, Heppner FL, McDonald DR, Lacombe D, Stupp R, Delorenzi M, Hegi ME, *MGMT* methylation analysis of glioblastoma on the Infinium methylation BeadChip identifies two distinct CpG regions associated with gene silencing and outcome, yielding a prediction model for comparisons across datasets, tumor grades, and CIMP-status. Acta Neuropathol. 124, 547–560 (2012). [PubMed: 22810491]

22. Erdem-Eraslan L, Gravendeel LA, de Rooi J, Eilers PHC, Idbaih A, Spliet WGM, den Dunnen WFA, Teepen JL, Wesseling P, Sillevis Smitt PAE, Kros JM, Gorlia T, van den Bent MJ, French PJ, Intrinsic molecular subtypes of glioma are prognostic and predict benefit from adjuvant procarbazine, lomustine, and vincristine chemotherapy in combination with other prognostic factors in anaplastic oligodendroglial brain tumors: A report from EORTC study 26951. J. Clin. Oncol 31, 328–336 (2013). [PubMed: 23269986]

23. Louis DN, Perry A, Reifenberger G, von Deimling A, Figarella-Branger D, Cavenee WK, Ohgaki H, Wiestler OD, Kleihues P, Ellison DW, The 2016 World Health Organization Classification of Tumors of the Central Nervous System: A summary. Acta Neuropathol. 131, 803–820 (2016). [PubMed: 27157931]

24. Ceccarelli M, Barthel FP, Malta TM, Sabedot TS, Salama SR, Murray BA, Morozova O, Newton Y, Radenbaugh A, Pagnotta SM, Anjum S, Wang J, Manyam G, Zoppoli P, Ling S, Rao AA, Grifford M, Cherniack AD, Zhang H, Poisson L, Carlotti CG Jr., da Cunha DP, Rao A, Mikkelsen T, Lau CC, Yung WKA, Rabadan R, Huse J, Brat DJ, Lehman NL, Barnholtz-Sloan JS, Zheng S, Hess K, Rao G, Meyerson M, Beroukhim R, Cooper L, Akbani R, Wrensch M, Haussler D, Aldape KD, Laird PW, Gutmann DH; TCGA Research Network, Noushmehr H, Iavarone A, Verhaak RGW, Molecular profiling reveals biologically discrete subsets and pathways of progression in diffuse glioma. Cell 164, 550–563 (2016). [PubMed: 26824661]

25. von Deimling A, Bender B, Jahnke R, Waha A, Kraus J, Albrecht S, Wellenreuther R, Faßbender F, Nagel J, Menon AG, Louis DN, Lenartz D, Schramm J, Wiestler OD, Loci associated with malignant progression in astrocytomas: A candidate on chromosome 19q. Cancer Res. 54, 1397–1401 (1994). [PubMed: 8137236]

26. Smith JS, Alderete B, Minn Y, Borell TJ, Perry A, Mohapatra G, Hosek SM, Kimmel D, O'Fallon J, Yates A, Feuerstein BG, Burger PC, Scheithauer BW, Jenkins RB, Localization of common deletion regions on 1p and 19q in human gliomas and their association with histological subtype. Oncogene 18, 4144–4152 (1999). [PubMed: 10435596]

27. Nakamura M, Yang F, Fujisawa H, Yonekawa Y, Kleihues P, Ohgaki H, Loss of heterozygosity on chromosome 19 in secondary glioblastomas. J. Neuropathol. Exp. Neurol 59, 539–543 (2000). [PubMed: 10850866]

28. Weller M, Felsberg J, Hartmann C, Berger H, Steinbach JP, Schramm J, Westphal M, Schackert G, Simon M, Tonn JC, Heese O, Krex D, Nikkhah G, Pietsch T, Wiestler O, Reifenberger G, von Deimling A, Loeffler M, Molecular predictors of progression-free and overall survival in patients with newly diagnosed glioblastoma: A prospective translational study of the German Glioma Network. J. Clin. Oncol 27, 5743–5750 (2009). [PubMed: 19805672]

29. Burton EC, Lamborn KR, Feuerstein BG, Prados M, Scott J, Forsyth P, Passe S, Jenkins RB, Aldape KD, Genetic aberrations defined by comparative genomic hybridization distinguish long-term from typical survivors of glioblastoma. Cancer Res. 62, 6205–6210 (2002). [PubMed: 12414648]

30. Beroukhim R, Getz G, Nghiemphu L, Barretina J, Hsueh T, Linhart D, Vivanco I, Lee JC, Huang JH, Alexander S, Du J, Kau T, Thomas RK, Shah K, Soto H, Perner S, Prensner J, Debiasi RM, Demichelis F, Hatton C, Rubin MA, Garraway LA, Nelson SF, Liau L, Mischel PS, Cloughesy TF, Meyerson M, Golub TA, Lander ES, Mellinghoff IK, Sellers WR, Assessing the significance of

chromosomal aberrations in cancer: Methodology and application to glioma. Proc. Natl. Acad. Sci. U.S.A 104, 20007–20012 (2007). [PubMed: 18077431]

31. Lee DW, Ramakrishnan D, Valenta J, Parney IF, Bayless KJ, Sitcheran R, The NF-κB RelB protein is an oncogenic driver of mesenchymal glioma. PLOS ONE 8, e57489 (2013). [PubMed: 23451236]
32. Bowman RL, Wang Q, Carro A, Verhaak RGW, Squatrito M, GlioVis data portal for visualization and analysis of brain tumor expression datasets. Neuro Oncol. 19, 139–141 (2017). [PubMed: 28031383]
33. Mani SA, Guo W, Liao M-J, Eaton E. Ng., Ayyanan A, Zhou AY, Brooks M, Reinhard F, Zhang C, Shipitsin M, Campbell LL, Polyak K, Brisken C, Yang J, Weinberg RA, The epithelial-mesenchymal transition generates cells with properties of stem cells. Cell 133, 704–715 (2008). [PubMed: 18485877]
34. Manavalan B, Basith S, Choi Y-M, Lee G, Choi S, Structure-function relationship of cytoplasmic and nuclear IκB proteins: An in silico analysis. PLOS ONE 5, e15782 (2010). [PubMed: 21203422]
35. Masereel B, Rolin S, Abbate F, Scozzafava A, Supuran CT, Carbonic anhydrase inhibitors: Anticonvulsant sulfonamides incorporating valproyl and other lipophilic moieties. J. Med. Chem 45, 312–320 (2002). [PubMed: 11784136]
36. Said HM, Supuran CT, Hageman C, Staab A, Polat B, Katzer A, Scozzafava A, Anacker J, Flentje M, Vordermark D, Modulation of carbonic anhydrase 9 (CA9) in human brain cancer. Curr. Pharm. Des 16, 3288–3299 (2010). [PubMed: 20819065]
37. Said HM, Hagemann C, Carta F, Katzer A, Polat B, Staab A, Scozzafava A, Anacker J, Vince GH, Flentje M, Supuran CT, Hypoxia induced CA9 inhibitory targeting by two different sulfonamide derivatives including acetazolamide in human glioblastoma. Bioorg. Med. Chem 21, 3949–3957 (2013). [PubMed: 23706268]
38. Das A, Banik NL, Ray SK, Modulatory effects of acetazolomide and dexamethasone on temozolomide-mediated apoptosis in human glioblastoma T98G and U87MG cells. Cancer Invest. 26, 352–358 (2008). [PubMed: 18443955]
39. Amiri A, Uyen Le P, Moquin A, Machkalyan G, Petrecca K, Gillard JW, Yoganathan N, Maysinger D, Inhibition of carbonic anhydrase IX in glioblastoma multiforme. Eur. J. Pharm. Biopharm 109, 81–92 (2016). [PubMed: 27702686]
40. Supuran CT, Acetazolamide for the treatment of idiopathic intracranial hypertension. Expert Rev. Neurother 15, 851–856 (2015). [PubMed: 26154918]
41. Boyd NH, Walker K, Fried J, Hackney JR, McDonald PC, Benavides GA, Spina R, Audia A, Scott SE, Libby CJ, Tran AN, Bevensee MO, Griguer C, Nozell S, Gillespie GY, Nabors B, Bhat KP, Bar EE, Darley-Usmar V, Xu B, Gordon E, Cooper SJ, Dedhar S, Hjelmeland AB, Addition of carbonic anhydrase 9 inhibitor SLC-0111 to temozolomide treatment delays glioblastoma growth in vivo. JCI Insight 2, e92928 (2017).
42. Wu J, Li L, Jiang G, Zhan H, Wang N, B-cell CLL/lymphoma 3 promotes glioma cell proliferation and inhibits apoptosis through the oncogenic STAT3 pathway. Int. J. Oncol 49, 2471–2479 (2016). [PubMed: 27748795]
43. Johnson BE, Mazor T, Hong C, Barnes M, Aihara K, McLean CY, Fouse SD, Yamamoto S, Ueda H, Tatsuno K, Asthana S, Jalbert LE, Nelson SJ, Bollen AW, Gustafson WC, Charron E, Weiss WA, Smirnov IV, Song JS, Olshen AB, Cha S, Zhao Y, Moore RA, Mungall AJ, Jones SJ, Hirst M, Marra MA, Saito N, Aburatani H, Mukasa A, Berger MS, Chang SM, Taylor BS, Costello JF, Mutational analysis reveals the origin and therapy-driven evolution of recurrent glioma. Science 343, 189–193 (2014). [PubMed: 24336570]
44. Muller FL, Colla S, Aquilanti E, Manzo VE, Genovese G, Lee J, Eisenson D, Narurkar R, Deng P, Nezi L, Lee MA, Hu B, Hu J, Sahin E, Ong D, Fletcher-Sananikone E, Ho D, Kwong L, Brennan C, Wang YA, Chin L, DePinho RA, Passenger deletions generate therapeutic vulnerabilities in cancer. Nature 488, 337–342 (2012). [PubMed: 22895339]
45. Nijhawan D, Zack TI, Ren Y, Strickland MR, Lamothe R, Schumacher SE, Tsherniak A, Besche HC, Rosenbluh J, Shehata S, Cowley GS, Weir BA, Goldberg AL, Mesirov JP, Root DE, Bhatia SN, Beroukhim R, Hahn WC, Cancer vulnerabilities unveiled by genomic loss. Cell 150, 842–854 (2012). [PubMed: 22901813]

46. Cairncross JG, Ueki K, Zlatescu MC, Lisle DK, Finkelstein DM, Hammond RR, Silver JS, Stark PC, Macdonald DR, Ino Y, Ramsay DA, Louis DN, Specific genetic predictors of chemotherapeutic response and survival in patients with anaplastic oligodendrogliomas. J. Natl. Cancer Inst 90, 1473–1479 (1998). [PubMed: 9776413]
47. Brat DJ, Seiferheld WF, Perry A, Hammond EH, Murray KJ, Schulsinger AR, Mehta MP, Curran WJ; Radiation Therapy Oncology Group, Analysis of 1p, 19q, 9p, and 10q as prognostic markers for high-grade astrocytomas using fluorescence in situ hybridization on tissue microarrays from Radiation Therapy Oncology Group trials. Neuro Oncol. 6, 96–103 (2004). [PubMed: 15134623]
48. Smith JS, Tachibana I, Pohl U, Lee HK, Thanarajasingam U, Portier BP, Ueki K, Ramaswamy S, Billings SJ, Mohrenweiser HW, Louis DN, Jenkins RB, A transcript map of the chromosome 19q-arm glioma tumor suppressor region. Genomics 64, 44–50 (2000). [PubMed: 10708517]
49. Bettegowda C, Agrawal N, Jiao Y, Sausen M, Wood LD, Hruban RH, Rodriguez FJ, Cahill DP, McLendon R, Riggins G, Velculescu VE, Oba-Shinjo SM, Marie SKN, Vogelstein B, Bigner D, Yan H, Papadopoulos N, Kinzler KW, Mutations in *CIC* and *FUBP1* contribute to human oligodendroglioma. Science 333, 1453–1455 (2011). [PubMed: 21817013]
50. Shostak K, Zhang X, Hubert P, Göktuna SI, Jiang Z, Klevernic I, Hildebrand J, Roncarati P, Hennuy B, Ladang A, Somja J, Gothot A, Close P, Delvenne P, Chariot A, NF-κB-induced KIAA1199 promotes survival through EGFR signalling. Nat. Commun 5, 5232 (2014). [PubMed: 25366117]
51. Massoumi R, Kuphal S, Hellerbrand C, Haas B, Wild P, Spruss T, Pfeifer A, Fässler R, Bosserhoff AK, Down-regulation of CYLD expression by Snail promotes tumor progression in malignant melanoma. J. Exp. Med 206, 221–232 (2009). [PubMed: 19124656]
52. Wakefield AM, Soukupova J, Montagne A, Ranger JJ, French R, Muller WJ, Clarkson RWE, Bcl3 selectively promotes metastasis of ERBB2-driven mammary tumors. Cancer Res. 15, 745–755 (2013).
53. Viatour P, Bentires-Alj M, Chariot A, Deregowski V, de Leval L, Merville M-P, Bours V, NF-κB2/p100 induces Bcl-2 expression. Leukemia 17, 1349–1356 (2003). [PubMed: 12835724]
54. Kashatus D, Cogswell P, Baldwin AS, Expression of the Bcl-3 proto-oncogene suppresses p53 activation. Genes Dev. 20, 225–235 (2006). [PubMed: 16384933]
55. Mansour NM, Bernal GM, Wu L, Crawley CD, Cahill KE, Voce DJ, Balyasnikova IV, Zhang W, Spretz R, Nunez L, Larsen GF, Weichselbaum RR, Yamini B, Decoy receptor DcR1 is induced in a p50/Bcl3–dependent manner and attenuates the efficacy of temozolomide. Cancer Res. 75, 2039–2048 (2015). [PubMed: 25808868]
56. Haapasalo J, Nordfors K, Järvelä S, Bragge H, Rantala I, Parkkila A-K, Haapasalo H, Parkkila S, Carbonic anhydrase II in the endothelium of glial tumors: A potential target for therapy. Neuro Oncol. 9, 308–313 (2007). [PubMed: 17435181]
57. Teicher BA, Liu SD, Liu JT, Holden SA, Herman TS, A carbonic anhydrase inhibitor as a potential modulator of cancer therapies. Anticancer Res. 13, 1549–1556 (1993). [PubMed: 8239534]
58. Bayat Mokhtari R, Baluch N, Ka Hon Tsui M, Kumar S, Homayouni TS, Aitken K, Das B, Baruchel S, Yeger H, Acetazolamide potentiates the anti-tumor potential of HDACi, MS-275, in neuroblastoma. BMC Cancer 17, 156 (2017). [PubMed: 28235409]
59. Neri D, Supuran CT, Interfering with pH regulation in tumours as a therapeutic strategy. Nat. Rev. Drug Discov 10, 767–777 (2011). [PubMed: 21921921]
60. Yamini B, Yu X, Dolan ME, Wu MH, Darga TE, Kufe DW, Weichselbaum RR, Inhibition of nuclear factor-κB activity by temozolomide involves O^6-methylguanine–induced inhibition of p65 DNA binding. Cancer Res. 67, 6889–6898 (2007). [PubMed: 17638900]
61. Tsen AR, Long PM, Driscoll HE, Davies MT, Teasdale BA, Penar PL, Pendlebury WW, Spees JL, Lawler SE, Viapiano MS, Jaworski DM, Triacetin-based acetate supplementation as a chemotherapeutic adjuvant therapy in glioma. Int. J. Cancer 134, 1300–1310 (2014). [PubMed: 23996800]
62. Nandhu MS, Hu B, Cole SE, Erdreich-Epstein A, Rodriguez-Gil DJ, Viapiano MS, Novel paracrine modulation of Notch–DLL4 signaling by fibulin-3 promotes angiogenesis in high-grade gliomas. Cancer Res. 74, 5435–5448 (2014). [PubMed: 25139440]

63. Lee J, Kotliarova S, Kotliarov Y, Li A, Su Q, Donin NM, Pastorino S, Purow BW, Christopher N, Zhang W, Park JK, Fine HA, Tumor stem cells derived from glioblastomas cultured in bFGF and EGF more closely mirror the phenotype and genotype of primary tumors than do serum-cultured cell lines. Cancer Cell 9, 391–403 (2006). [PubMed: 16697959]
64. Lan X, Jörg DJ, Cavalli FMG, Richards LM, Nguyen LV, Vanner RJ, Guilhamon P, Lee L, Kushida MM, Pellacani D, Park NI, Coutinho FJ, Whetstone H, Selvadurai HJ, Che C, Luu B, Carles A, Moksa M, Rastegar N, Head R, Dolma S, Prinos P, Cusimano MD, Das S, Bernstein M, Arrowsmith CH, Mungall AJ, Moore RA, Ma Y, Gallo M, Lupien M, Pugh TJ, Taylor MD, Hirst M, Eaves CJ, Simons BD, Dirks PB, Fate mapping of human glioblastoma reveals an invariant stem cell hierarchy. Nature 549, 227–232 (2017). [PubMed: 28854171]
65. Hu Y, Smyth GK, ELDA: Extreme limiting dilution analysis for comparing depleted and enriched populations in stem cell and other assays. J. Immunol. Methods 347, 70–78 (2009). [PubMed: 19567251]
66. Gravendeel LAM, Kouwenhoven MCM, Gevaert O, de Rooi JJ, Stubbs AP, Duijm JE, Daemen A, Bleeker FE, Bralten LBC, Kloosterhof NK, De Moor B, Eilers PHC, van der Spek PJ, Kros JM, Sillevis Smitt PAE, van den Bent MJ, French PJ, Intrinsic gene expression profiles of gliomas are a better predictor of survival than histology. Cancer Res. 69, 9065–9072 (2009). [PubMed: 19920198]
67. Freije WA, Castro-Vargas FE, Fang Z, Horvath S, Cloughesy T, Liau LM, Mischel PS, Nelson SF, Gene expression profiling of gliomas strongly predicts survival. Cancer Res. 64, 6503–6510 (2004). [PubMed: 15374961]
68. Joy A, Ramesh A, Smirnov I, Reiser M, Misra A, Shapiro WR, Mills GB, Kim S, Feuerstein AG, AKT pathway genes define 5 prognostic subgroups in glioblastoma. PLOS ONE 9, e100827 (2014). [PubMed: 24984002]
69. Lee Y, Scheck AC, Cloughesy TF, Lai A, Dong J, Farooqi HK, Liau LM, Horvath S, Mischel PS, Nelson SF, Gene expression analysis of glioblastomas identifies the major molecular basis for the prognostic benefit of younger age. BMC Med. Genomics 1 52 (2008). [PubMed: 18940004]
70. Rich JN, Hans C, Jones B, Iversen ES, McLendon RE, Ahmed Rasheed BK, Dobra A, Dressman HK, Bigner DD, Nevins JR, West M, Gene expression profiling and genetic markers in glioblastoma survival. Cancer Res. 65, 4051–4058 (2005). [PubMed: 15899794]
71. Petalidis LP, Oulas A, Backlund M, Wayland MT, Liu L, Plant K, Happerfield L, Freeman TC, Poirazi P, Collins VP, Improved grading and survival prediction of human astrocytic brain tumors by artificial neural network analysis of gene expression microarray data. Mol. Cancer Ther 7, 1013–1024 (2008). [PubMed: 18445660]
72. Turcan S, Rohle D, Goenka A, Walsh LA, Fang F, Yilmaz E, Campos C, Fabius AWM, Lu C, Ward PS, Thompson CB, Kaufman A, Guryanova O, Levine R, Heguy A, Viale A, Morris LGT, Huse JT, Mellinghoff IK, Chan TA, IDH1 mutation is sufficient to establish the glioma hypermethylator phenotype. Nature 483, 479–483 (2012). [PubMed: 22343889]

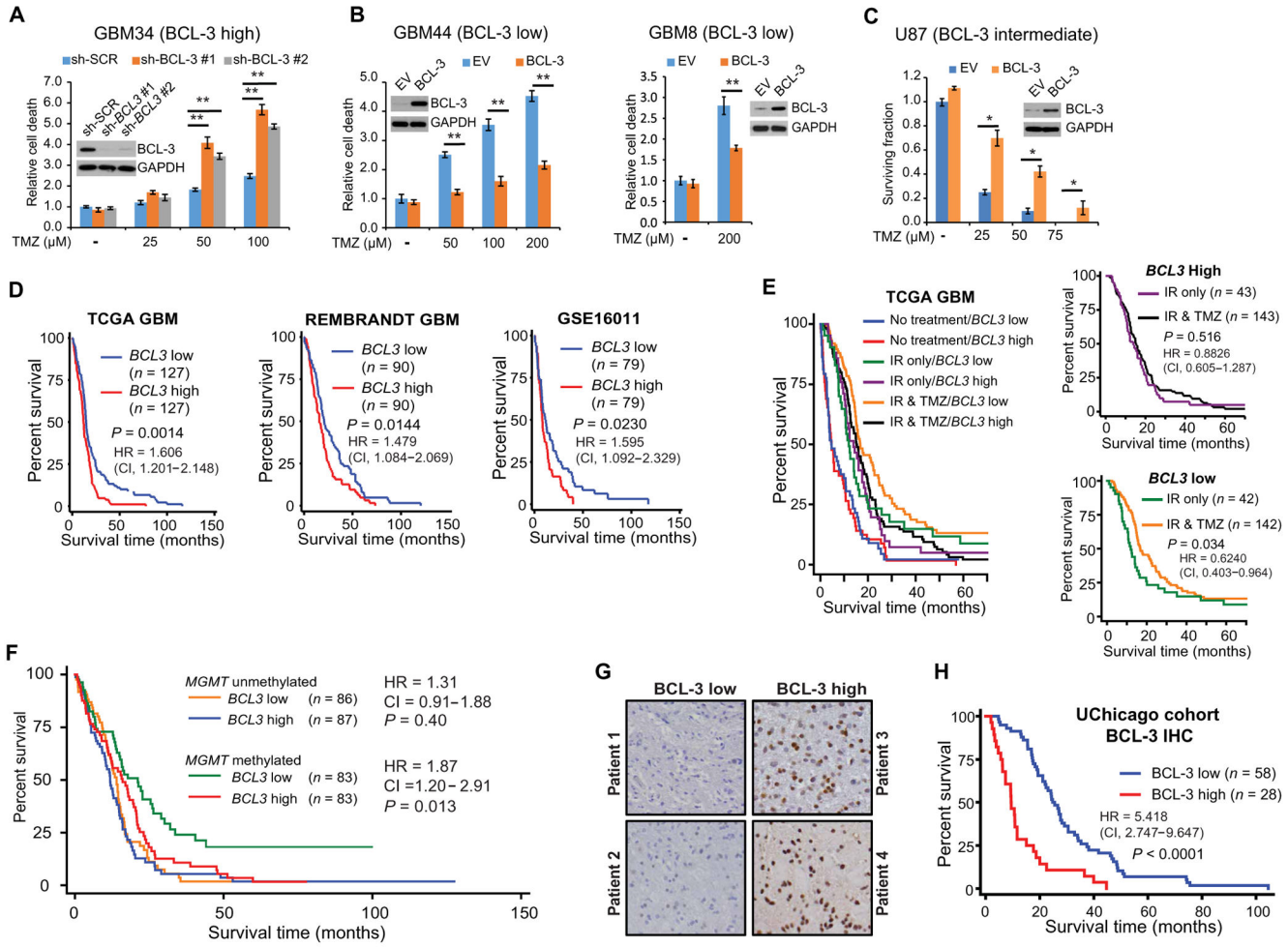

Fig. 1. *BCL3* predicts response to alkylating chemotherapy in GBM.

(**A** and **B**) Trypan blue assays in GSCs expressing the indicated construct treated with TMZ (72 hours). Data show fold change in percent dead cells relative to cells expressing a scrambled RNA sequence (sh-SCR), or empty vector (EV), treated with vehicle, ± SD (n = 3). Inset: Immunoblotting (IB) with anti–BCL-3. (**C**) Clonogenic assay in U87 cells stably expressing BCL-3 or EV treated with vehicle or TMZ. Data show mean value relative to vehicle ± SD (n = 3). GAPDH, glyceraldehyde-3-phosphate dehydrogenase. (**D** to **F**) Kaplan-Meier overall survival curves in GBM patients. (D) Survival based on median mRNA expression (REMBRANDT and GSE16011) and upper and lower quartile (TCGA). (E) TCGA GBM patients separated by median *BCL3* expression and treatment modality. n = 490 patients total: no treatment, IR alone, and IR + TMZ; inset graphs: IR versus IR + TMZ in patients with high or low *BCL3* mRNA (median cutoff). (F) TCGA GBM patients separated by median *MGMT* promoter methylation and median *BCL3* expression. (**G**) Representative IHC staining for BCL-3 in GBM. (**H**) Survival curves in GBM patients separated by BCL-3 IHC staining. Kaplan-Meier curves analyzed by the log-rank test. *P < 0.05 and **P < 0.01.

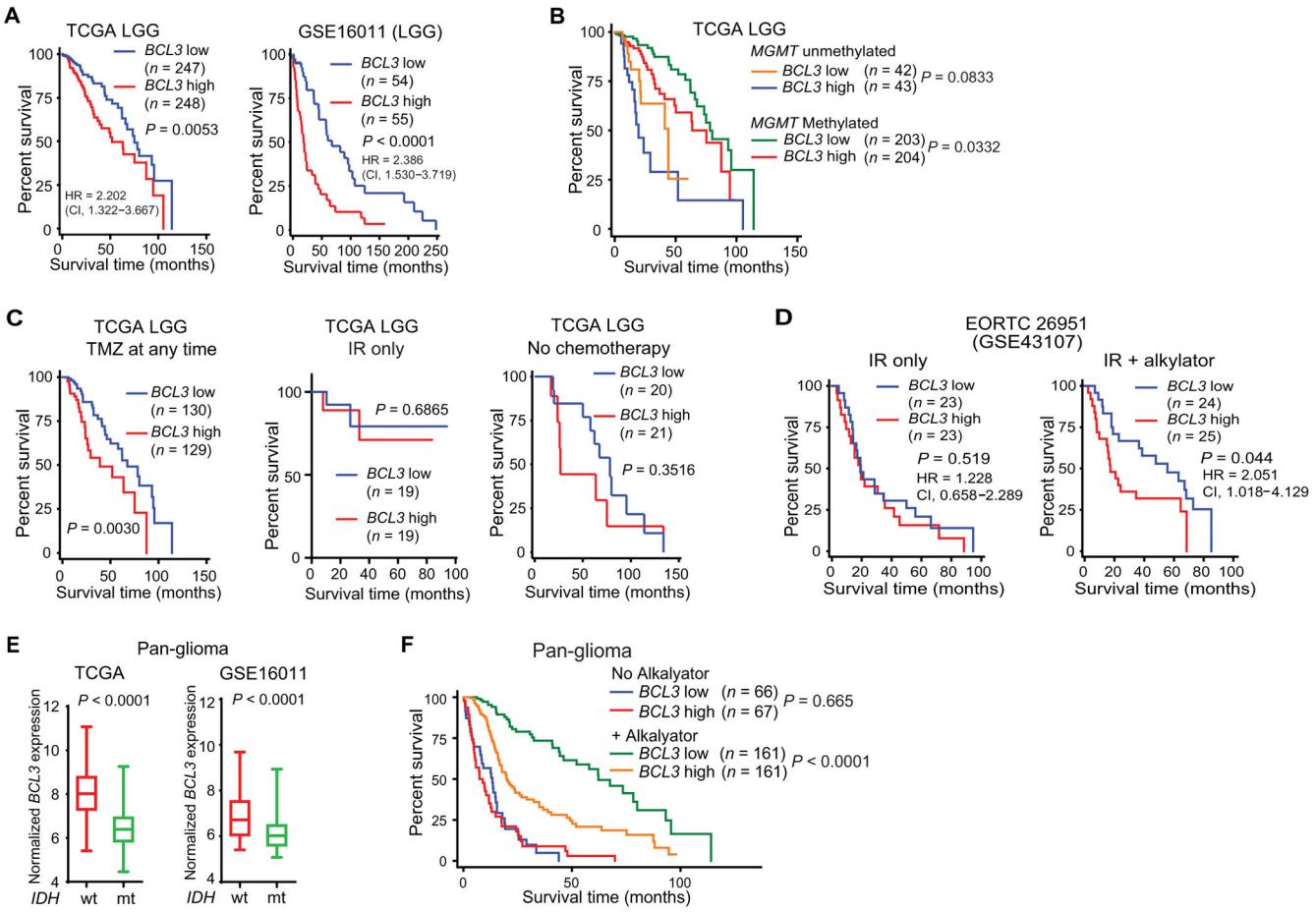

Fig. 2. *BCL3* is relevant in LGGs and pan-glioma patients.

(**A** and **B**) Survival curves from (A) LGG data sets separated by median *BCL3* expression and (B) TCGA LGG patients separated by median *BCL3* expression and median *MGMT* promoter methylation. (**C**) Survival curves in TCGA LGG patients based on median *BCL3* expression and treatment ($n = 338$ patients total). For patients treated with TMZ, 202 received only TMZ, and 57 received TMZ and PCV. No chemotherapy group includes patients with and without IR. IR alone patients received no alkylating agents. (**D**) Survival curves in EORTC 26951 based on median *BCL3* expression. Patients were separated by treatment modality into those treated with IR alone versus IR + alkylating chemotherapy. (**E**) *BCL3* mRNA expression in pan-glioma patients based on *IDH1* mutation status in the indicated data set. For TCGA: *IDH1*-wt, $n = 184$; *IDH1*-mt, $n = 406$. For GSE16011: *IDH1*-wt, $n = 143$; *IDH1*-mt, $n = 83$. (**F**) Survival curves in TCGA pan-glioma patients separated by median *BCL3* expression and by alkylating chemotherapy treatment (yes/no). Kaplan-Meier curves analyzed by the log-rank test.

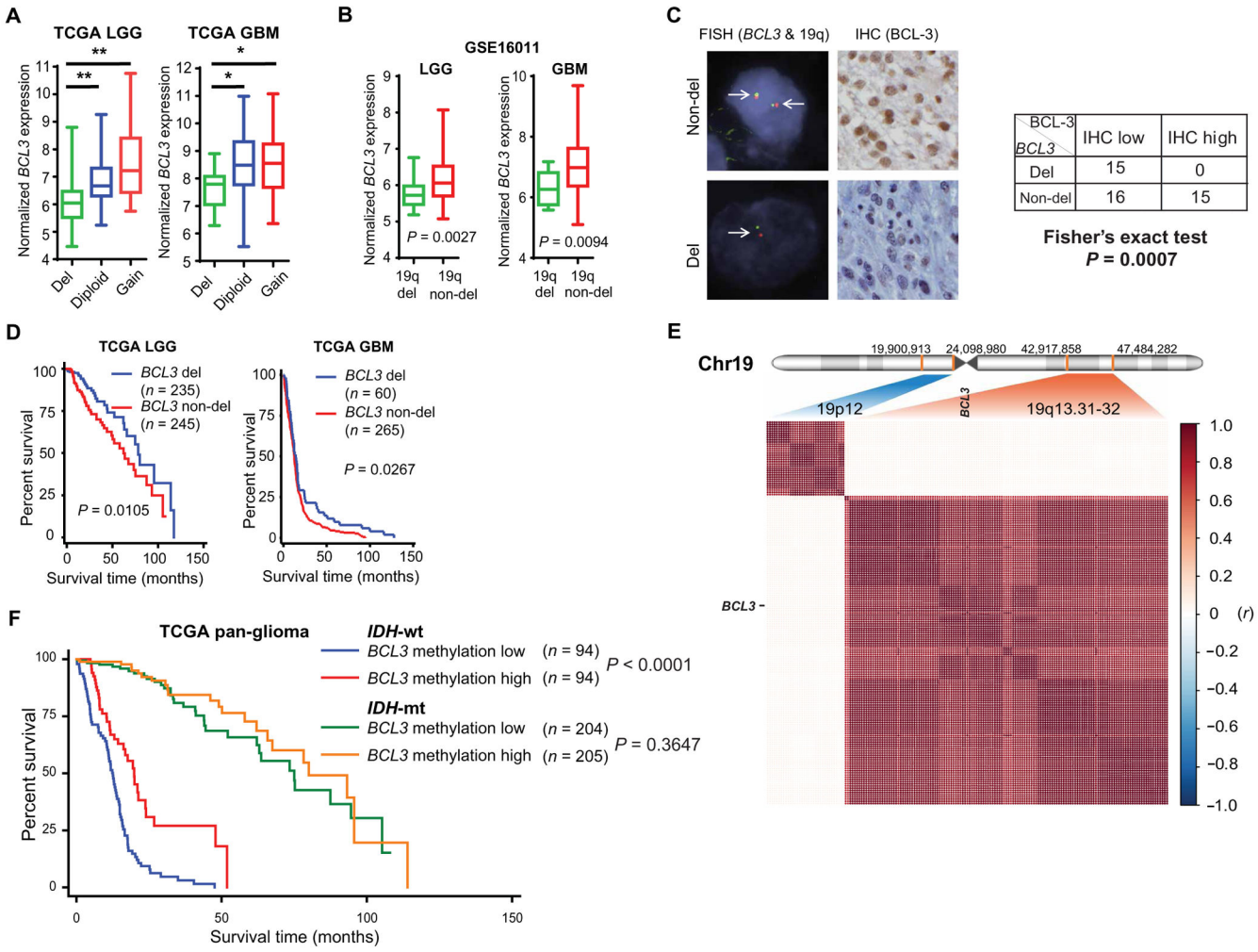

Fig. 3. Loss of *BCL3* is a passenger event associated with improved survival.

(**A**) Relationship between *BCL3* expression [on RNA sequencing (RNA-seq)] and *BCL3* CN in TCGA LGG and GBM. In LGG, del: $n = 169$; diploid: $n = 155$; gain: $n = 16$. In GBM, del: $n = 17$; diploid: $n = 89$; gain: $n = 39$. (**B**) *BCL3* expression in LGG and GBM tumors in relation to tumor 19q deletion status [determined by microsatellite polymerase chain reaction (PCR)]. LGG: del, $n = 40$; non-del, $n = 33$. GBM: del, $n = 12$; non-del, $n = 58$. (**C**) Representative FISH images using *BCL3* and 19q specific probes (left) and BCL-3 IHC staining (high and low, right) in human gliomas. Table shows number of tumors in each category, two-sided Fisher's exact test. (**D**) Kaplan-Meier curves in LGG and GBM patients based on *BCL3* CN (with and without deletion). (**E**) Correlogram showing correlation (r, y axis) between CN of genes from the indicated regions of chromosome 19 (Chr19) in $n = 514$ TCGA LGG patients. For 19q13.31-32 (Chr19:42,917,858 to 47,484,282), there are 171 genes in a span of 4.5 Mbp (million base pairs); 139 of these genes have CN data available for analysis. The nearest 19p band (19p12) was used as a reference. For 19p12 (Chr19: 19,900,913 to 24,098,980), there are 59 genes in the 4.2-Mbp region, of which 36 have CN data. Location of *BCL3* shown. (**F**) Survival in TCGA pan-glioma patients based on median

BCL3 promoter methylation and *IDH1* mutation status. Pearson coefficient (r) analyzed by two-sided Student's t test. *$P < 0.003$ and **$P < 0.0002$.

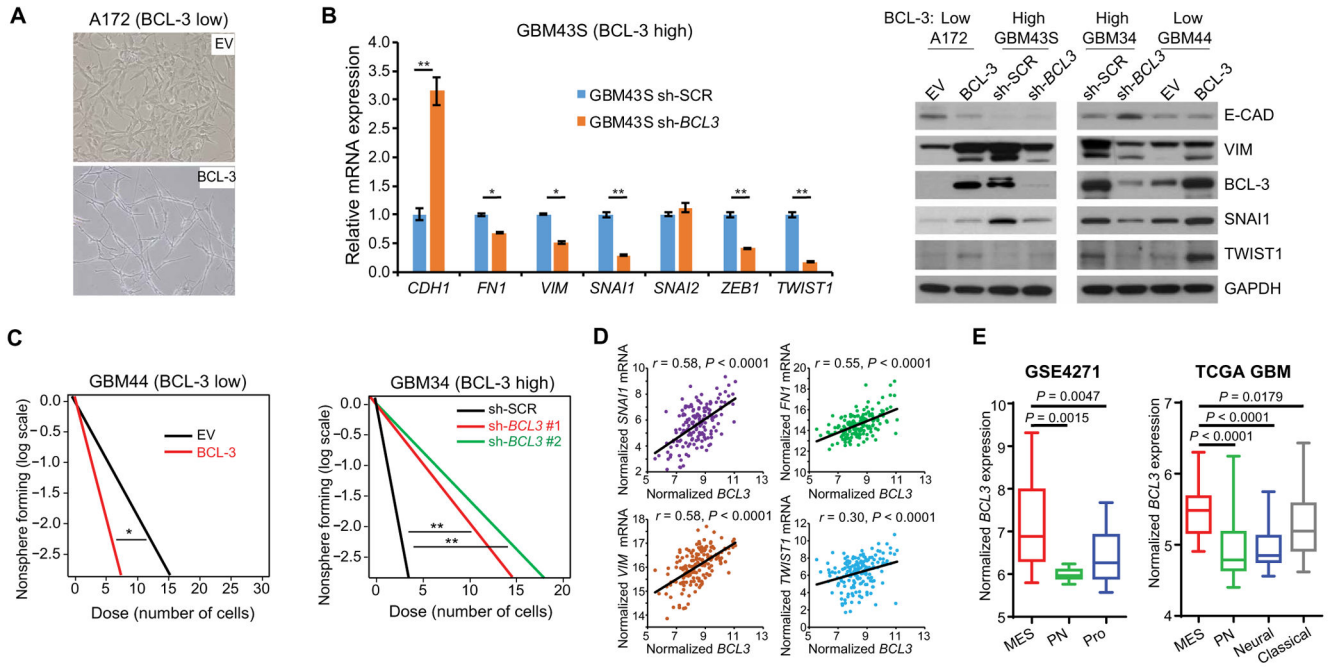

Fig. 4. BCL-3 induces mesenchymal differentiation.

(**A**) Photomicrograph of A172 cells stably expressing BCL-3 or EV (×20 magnification). (**B**) Quantitative PCR (left) and representative immunoblot (right) of mesenchymal markers in GSCs and GBM cells. qPCR data show mean value relative to *GAPDH* normalized to sh-SCR ± SD ($n = 3$). (**C**) Limiting dilution neurosphere assays in GBM44 and GBM34 GSCs expressing the indicated constructs ($n = 2$ biologic replicates). (**D**) Correlation between mesenchymal markers and *BCL3* mRNA in TCGA GBM samples ($n = 166$ for all genes). (**E**) *BCL3* mRNA expression in GBM molecular subtypes. Phillips (left) and Verhaak (right) classification schemes. For GSE4271: MES, $n = 22$; PN, $n = 9$; Proliferative (Pro), $n = 24$. For TCGA: MES, $n = 53$; Classical, $n = 37$; Neural, $n = 24$; PN, $n = 53$. *$P < 0.05$ and **$P < 0.01$. Pearson correlation analyzed by two-sided Student's *t* test.

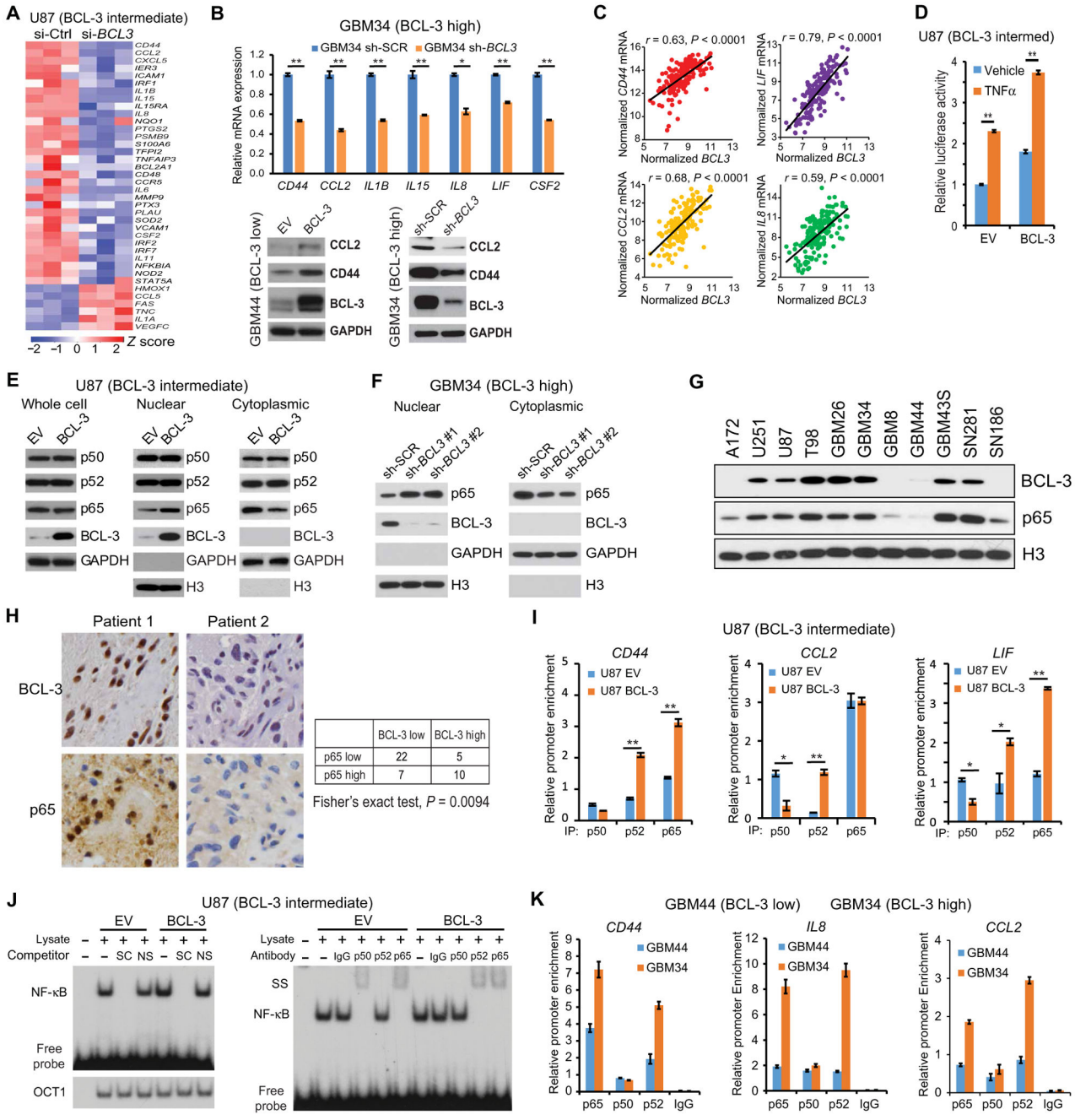

Fig. 5. BCL-3 promotes p65 nuclear translocation and NF-κB dimer exchange.

(**A**) Heatmap representing expression of all MES-specific NF-κB target genes [identified in (10)] in microarray analysis of U87 cells expressing si-control (Ctrl) or si-*BCL3*, performed using three separate biological samples. *Z* score normalized expression is graded by color. (**B**) qPCR (upper) of MES-specific genes in GBM34 GSCs. Data show mean value relative to *GAPDH* normalized to sh-SCR ± SD ($n = 3$). Bottom: Representative immunoblots in GBM44 and GBM34 GSCs expressing the indicated construct. (**C**) Correlation between MES-specific genes and *BCL3* mRNA in TCGA GBM samples ($n = 166$ for all genes). (**D**) Relative luciferase activity in U87 cells expressing BCL-3 or EV treated with TNFα (5

ng/ml) or vehicle (12 hours). Data show mean value, normalized to vehicle-treated EV, ± SD ($n = 4$). (**E**) Representative immunoblot using the indicated cellular fractions from U87 cells expressing HA-BCL-3 or EV. (**F**) Immunoblot analysis with the indicated antibody using cytoplasmic and nuclear extract from GBM34 GSCs expressing two separate sh-*BCL3* constructs or sh-SCR. Histone 3 (H3) antibody was used as nuclear loading control. (**G**) Representative immunoblot using nuclear fractions from the indicated GSCs and GBM cell lines. (**H**) Representative IHC images (left) of GBM samples from glioma TMAs showing nuclear p65 and BCL-3 staining in two patients. Table (right) shows numbers of tumors in each category. (**I**) ChIP qPCR in the indicated cells after IP. Data represent enrichment at the indicated promoter as a percentage of input ± SD ($n = 2$). (**J**) Representative electrophoretic mobility shift assay (EMSA) with CD44 κB probe using nuclear extracts from U87 cells expressing BCL-3 or EV. Supershift (SS) (right) and competition with specific (SC) or nonspecific (NS) probe (left); OCT1 binding confirms equal loading. (**K**) ChIP qPCR in GSCs after IP with the indicated antibodies. Data represent enrichment at the indicated promoter as a percentage of input ± SD ($n = 2$). *$P < 0.05$ and **$P < 0.01$. Pearson correlation analyzed by two-sided Student's *t* test. Significance in IHC was calculated using two-sided Fisher's exact test.

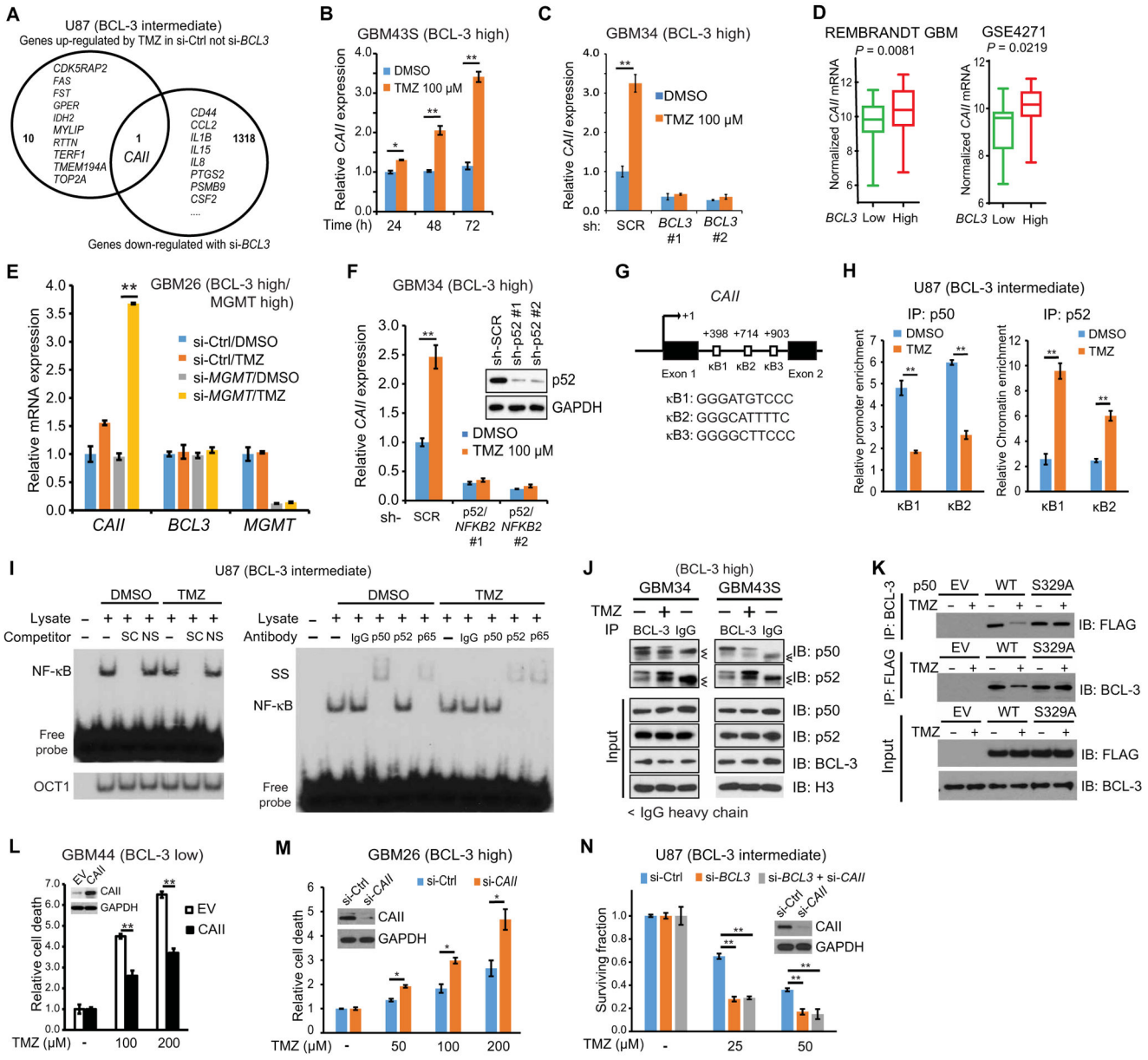

Fig. 6. CAII mediates BCL-3–dependent resistance to TMZ.

(**A**) Significantly ($P < 0.05$) altered transcripts in U87 cells expressing si-*BCL3* or si-control treated with TMZ (100 μM) or vehicle (24 hours). (**B**) *CAII* mRNA expression relative to *GAPDH* in GBM43S GSCs treated with TMZ ($n = 3$). (**C**) *CAII* mRNA in GBM34 GSCs expressing sh-*BCL3* constructs or sh-control treated with vehicle or TMZ (48 hours) ($n = 3$). (**D**) *CAII* mRNA expression in patients from the indicated data set with lower and upper 33% *BCL3* expression. REMBRANDT, $n = 61$ per group; GSE4271, $n = 20$ per group. (**E**) Expression of *CAII, BCL3*, and *MGMT* mRNA in GBM26 GSCs that express high MGMT (see fig. S7K) transfected with si-MGMT or si-control after treatment with 100 μM TMZ for 48 hours. Data show mean expression relative to *GAPDH* normalized to si-control, dimethyl sulfoxide (DMSO)–treated, ± SD ($n = 2$). (**F**) *CAII* expression relative to *GAPDH* in

GBM34 GSCs expressing sh-control or two separate sh-p52/*NFKB2* constructs after treatment with TMZ (48 hours). Data show mean value relative to *GAPDH* ± SD ($n = 3$). Inset: Immunoblot with anti-p52. (**G**) Location and sequence of putative human *CAII* κB sites. (**H**) ChIP qPCR in U87 cells treated with 100 μM TMZ or vehicle (24 hours). Data are normalized to immunoglobulin G (IgG) and represent enrichment as a percentage of input ± SD ($n = 2$). (**I**) Representative EMSA with κB2 probe in U87 nuclear lysate treated as in (H). Supershift (SS) (right) and competition with specific (SC) or nonspecific (NS) probe (left). OCT1 binding confirms equal loading. (**J**) Co-IP in GBM34 and GBM43S GSCs (both BCL-3 high) after treatment with TMZ (100 μM, 24 hours). IP and IB were performed with the indicated antibodies. Arrowheads indicate IgG heavy chain band ($n = 2$). (**K**) Reciprocal co-IP in 293T cells expressing FLAG-p50-wt, FLAG-p50-S329A, or EV after treatment with vehicle or TMZ (100 μM, 24 hours) ($n = 2$). (**L** and **M**) Trypan blue assays in GBM44 GSCs expressing HA-CAII or EV (L) and GBM26 GSCs expressing si-CAII or si-control (M) treated with TMZ (72 hours). Data show fold change in percent dead cells relative to vehicle ± SD ($n = 3$). Insets: Immunoblots with anti-CAII antibody. (**N**) Clonogenic assay in U87 cells expressing si-control or si-*BCL3* with and without si-CAII treated with TMZ ($n = 3$). *$P < 0.05$ and **$P < 0.01$, two-sided Student's *t* test.

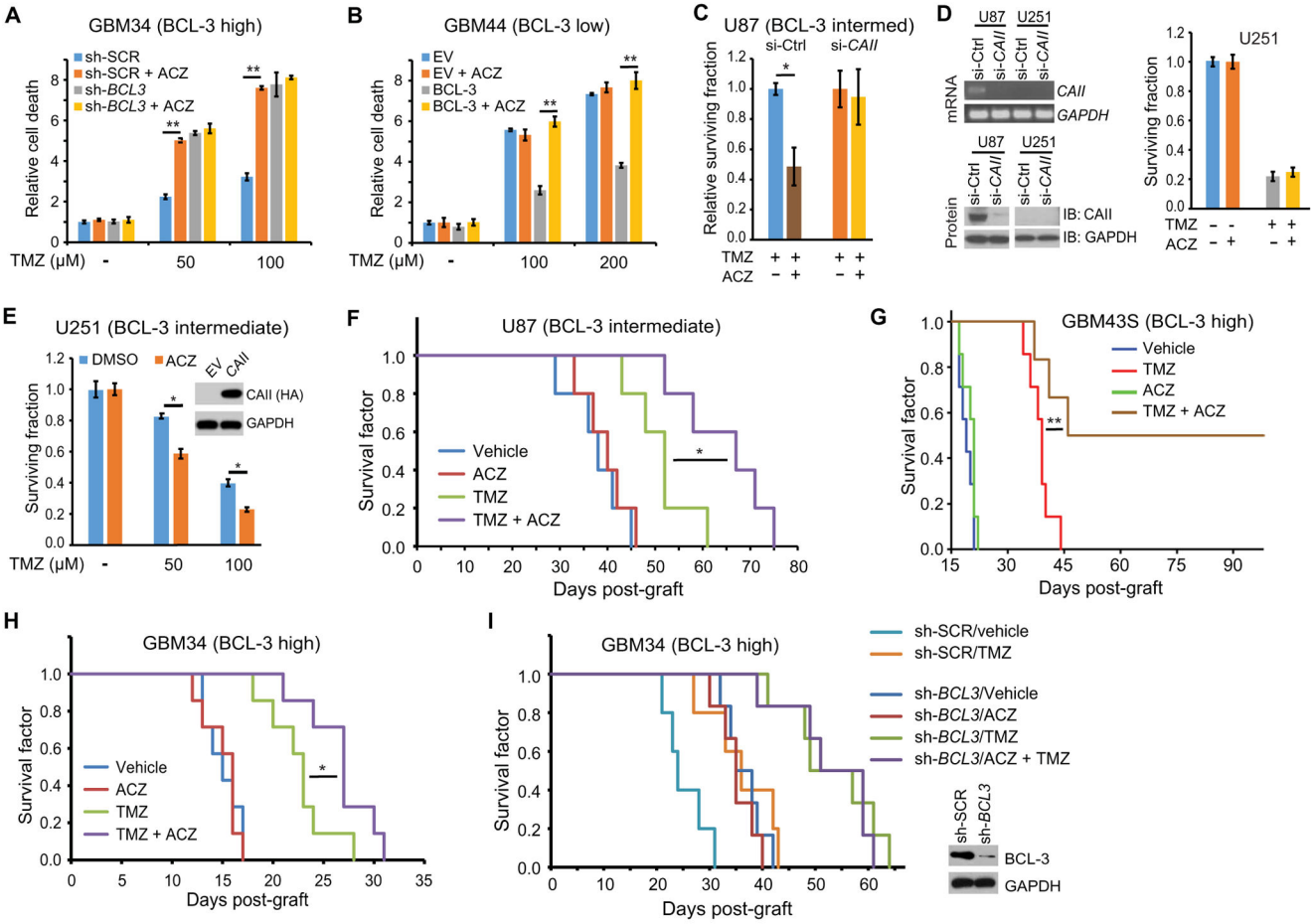

Fig. 7. ACZ chemosensitizes GBM xenografts to TMZ.

(**A** and **B**) Trypan blue assays at 72 hours in (A) GBM34 GSCs expressing sh-*BCL3* or sh-SCR or (B) GBM44 GSCs expressing BCL-3 or EV treated with TMZ and/or 100 μM ACZ as indicated. Data show fold change in percent dead cells relative to cells transfected with EV, or sh-SCR, treated with vehicle, ± SD ($n = 3$). (**C**) Clonogenic assay in U87 cells expressing si-CAII or si-control treated with 50 μM TMZ with or without 100 μM ACZ. Data show surviving fraction relative to TMZ alone ± SD ($n = 3$). (**D**) PCR analysis of *CAII* mRNA and immunoblot analysis of CAII protein in U87 and U251 cells expressing si-control or si-CAII. Clonogenic assay (right) in U251 cells treated with 100 μM TMZ and/or 100 μM ACZ ($n = 3$). (**E**) Clonogenic assay in U251 cells stably expressing CAII or EV treated with TMZ and/or 100 μM ACZ ($n = 3$). (**F**) Kaplan-Meier curves of mice bearing intracranial U87 tumors ($n = 5$ per group) treated with TMZ on days 5, 7, and 9 (5 mg/kg per dose) and/or ACZ on days 5 to 26 (15 mg/kg per day). (**G**) Kaplan-Meier curves of mice bearing intracranial GBM43S PDX ($n = 7$ per group) treated with TMZ on days 5, 7, and 9 (5 mg/kg per dose) and/or ACZ on days 5 to 26 (15 mg/kg per day). (**H**) Kaplan-Meier curves of mice bearing intracranial GBM34 PDX ($n = 7$ per group) treated with TMZ on days 5, 7, and 9 (10 mg/kg per dose) and/or ACZ on days 5 to 26 (15 mg/kg per day). (**I**) Kaplan-Meier curves of mice bearing intracranial GBM34 PDX tumors stably expressing either sh-*BCL3* ($n = 6$ per group) or sh-SCR ($n = 5$ per group) treated with TMZ on days 5,

7, and 9 (10 mg/kg per dose) and/or ACZ on days 5 to 26 (15 mg/kg per day). Inset: Immunoblot of cells from the indicated tumors. *$P < 0.05$ and **$P < 0.02$.

Table 1.

Cox regression analysis in TCGA GBM patients.

Covariate	Univariate regression			Multivariate regression		
	HR	95% CI	*P*	HR	95% CI	*P*
BCL3 expression	1.408	1.131–1.752	0.002	1.455	1.069–1.981	0.017
MGMT methylation	0.624	0.482–0.808	0.000	0.754	0.580–0.981	0.035
IDH1 mutation	0.232	0.075–0.724	0.012	0.490	0.153–1.573	0.231
Radiotherapy	0.357	0.287–0.445	0.000	0.424	0.307–0.585	0.000
Chemotherapy	0.576	0.471–0.705	0.000	0.650	0.492–0.860	0.003
Procurement method	1.155	0.864–1.543	0.330	1.055	0.734–1.516	0.773
Age	1.035	1.027–1.044	0.000	1.027	1.016–1.039	0.000

Table 2.
Cox regression analysis in TCGA LGG patients.

BCL3 expression is also significant with inclusion of grade into analysis ($P = 0.042$).

Covariate	Univariate regression		
	HR	95% CI	*P*
BCL3 expression	1.431	1.186–1.735	0.000
MGMT methylation	0.268	0.167–0.431	0.000
IDH1 mutation	0.103	0.062–0.173	0.000
1p/19q co-deletion	0.486	0.281–0.837	0.009
Grade (II or III)	3.554	2.194–5.758	0.000
Radiotherapy	0.404	0.202–0.807	0.010
Chemotherapy	0.219	0.068–0.706	0.011
Procurement method	1.402	0.911–2.159	0.125
Age	1.060	1.042–1.079	0.000
Covariate	**Multivariate regression**		
	HR	**95% CI**	***P***
BCL3 expression	1.374	1.096–1.722	0.006
MGMT methylation	0.685	0.363–1.293	0.243
IDH1 mutation	0.401	0.186–0.864	0.020
1p/19q co-deletion	0.646	0.339–1.229	0.183
Age	1.064	1.042–1.086	0.000

Table 3.

Cox regression analysis in TCGA pan-glioma patients.

Only patients with RNA-seq data included.

Covariate	Univariate regression			Multivariate regression		
	HR	95% CI	*P*	HR	95% CI	*P*
BCL3 expression	2.390	2.065–2.765	0.000	1.467	1.213–1.774	0.000
MGMT methylation	0.227	0.168–0.307	0.000	0.590	0.416–0.835	0.003
IDH1 mutation	0.073	0.051–0.103	0.000	0.309	0.176–0.541	0.000
1p/19q co-deletion	0.212	0.127–0.353	0.000	0.705	0.379–1.312	0.270
Age	1.070	1.058–1.080	0.000	1.052	1.037–1.066	0.000